Journal of Natural Disaster Science, Volume 4, Number 2, 1982, pp. 1–32

DRY DEBRIS FLOW OF PYROCLASTIC FALL DEPOSITS TRIGGERED BY THE 1978 IZU-OSHIMA-KINKAI EARTHQUAKE: THE "COLLAPSING" LANDSLIDE AT NANAMAWARI, MITAKA-IRIYA, SOUTHERN IZU PENINSULA

Masahiro CHIGIRA

Geology Department, Civil Engineering Laboratory, Central Research Institute of Electric Power Industry, Abiko City, Chiba

(Received 23 July and in revised from 14 December, 1982)

ABSTRACT

A peculiar "collapsing" landslide occurred at Nanamawari, Mitaka-iriya, on the Izu Peninsula during the 1978 Izu-Oshima-Kinkai earthquake. Field investigations showed the causes and phenomena connected with this slide. The landslide began on a slope of 25° with the sliding of scoria, soil and part of the paleosol. The sliding surface was formed within the upper part of the paleosol, probably in a weathered ash bed, several meters below the original surface of the slope.

During of transportation, the sliding materials disintergrated into dry debris and flowed onto the flat surface across the river, dashed against the opposite slope then rebounded and settled in a lobe-shaped deposit with lateral ridges and a distal mound.

The landslide continued less than 30 seconds, but its maximum velocity was more than 11.7 m/s. The basic causes of the landslide were insufficient lateral support by strata on the lower slope and a weak halloysite-rich paleosol in which the sliding surface formed. The landslide at Nanamawari is considered a special type of slide found in Japan.

1. INTRODUCTION

Severe damage was caused in the eastern part of the Izu Peninsula by the 1978 Izu-Oshima-Kinkai earthquake, magnitude 7.0, which occurred at $12^{h}24^{m}$ on 14 January 1978. The epicenter of the main shock was located at 34.8°N and 139.8°E [1]. Physical phenomena associated with the earthquake have been described in detail in the *Bulletin of the Earthquake Research Institute, University of Tokyo* (Vol. 53, 1978).

Peculiar "collapsing"* landslides took place in Mitaka-iriya, Kawazu-cho, about 25 km west of the epicenter during this earthquake as well as many small landslides and rockfalls over a large area of the eastern part of the Izu Peninsula (Fig. 1). The landslides in Mitaka-iriya aroused considerable research interest because they took place on rather gentle slopes and formed depositional bodies over exceptionally large areas in comparison to their rather narrow source areas.

The Izu Peninsula has Miocene Yugashima and Shirahama Groups as its basement rocks, and these are widely overlain by volcanics of Pliocene to Quaternary age. In the eastern part particularly, many monogenetic volcanoes have been formed during the last tens of thousands of years [2]. Four monogenetic volcanoes (Oike, Koike, Oike-Minami, and Hachiyama) lie west of Mitaka-iriya at which place the materials making up the slopes are mainly composed

* I have used "collapsing" to designate a landslide in which most of the material collapses then disintegrates into debris.

Note: Discussion open until 30 November, 1983.

KEY WORDS: Landslide, Dry debris flow, Earthquake, Pyroclastic fall deposits, Paleosol

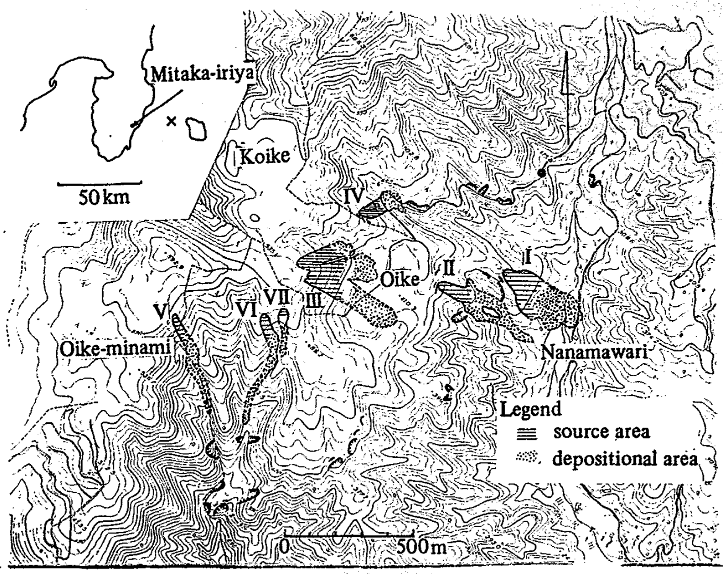

Fig. 1 Map of the distribution of landslides in Mitaka-iriya. For the numbers of the landslides refer to the text, section 3. The solid circle indicates the locality in Appendix B.

of pyroclastic fall deposits, scoria and ash. They probably came from eruptions of these volcanoes and show stratifications nearly parallel to the slope surfaces, except in areas where erosion has taken place.

The landslides in Mitaka-iriya began with the sliding of scoria, soil and a part of the paleosol on slopes of 15° to 30°. The sliding surface of each landslide was formed in the upper part of the paleosol, probably in weathered ash, several meters below the original surface of the slope. During transportation, the sliding material disintegrated into dry debris and flowed a distance of 100 to 300 m.

Most of the material on the slope slid down from the source area and was deposited on the river bed as well as on the flat area on either side of the river. The depositional area on the flat made a clearly defined lobe similar to that produced by the rock avalanche at Elm, Switzerland in 1881 [3]. Plants which grew on the original source surface were moved, but not mixed much with the debris; they ended on top of the deposits.

Landslides occurred at seven localities in Mitaka-iriya (Fig. 1). Of these, the landslide at Nanamawari (I in Fig. 1) which destroyed nine houses and killed seven people, has been studied in detail.

Before the slide at Nanamawari, similar disasterous collapsing landslides had taken place at many other localities during the 1949 Imaichi and 1968 off Tokachi (Tokachi-Oki) earthquakes. Their characteristics and causes, however, were not thoroughly determined as they have been for the Nanamawari slide in this study. The characteristics and causes of the landslide at Nanamawari and their general extension to collapsing landslides of pyroclastic fall deposits triggered by earthquakes are discussed.

2. THE COLLAPSING LANDSLIDE AT NANAMAWARI

2.1 Method of Study

No one who experienced the landslide directly survived. Moreover, its deposits were excavated immediately after the slide to rescue seven buried people. I began field work early in April, three months after the slide and used the following procedures to determine its characteristics and causes.

The nature of the slide area, immediately after the event, was reconstructed from interviews with residents who live in the civinity and by checking photographs taken by Mr. K. Tsuchiya on the day of and the day after the slide, ones taken by police officers from the Shimoda Police Station during excavation of the deposits, ones taken from the air by the Shimoda Forestry Office January 17th, and aerial photographs with a scale of 1:8,000 taken by the Aero Asahi Corporation on January 19th (Photo 1).

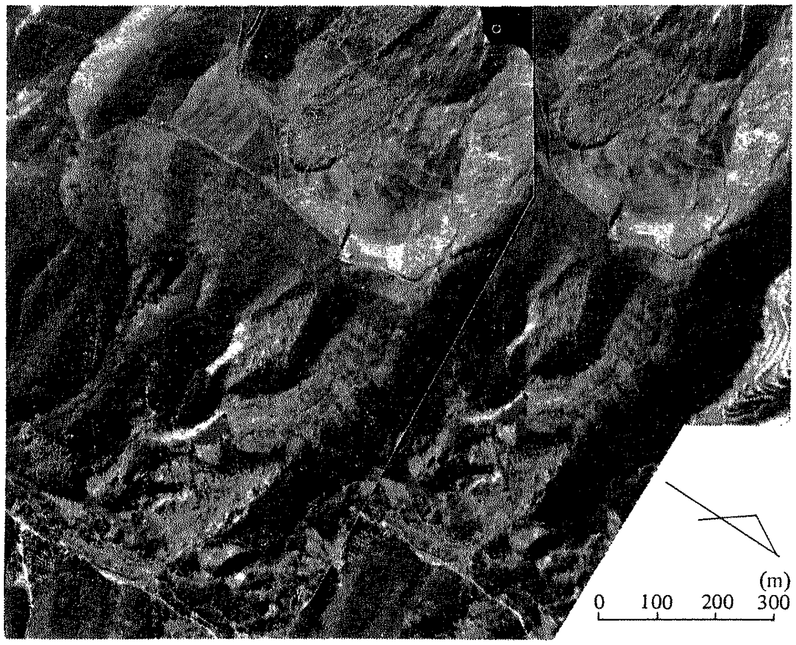

Photo 1 Stereo pair of aerial photographs of the landslides in Mitaka-iriya. The landslide at Nanamawari (I in Fig. 1) is in the east; landslides II and III are west of it. Landslide III formed very clear lobe-shaped deposits with a distal mound and lateral ridges. These photographs were taken by the Aero Asahi Corporation on January 19th, five days after the earthquake (photograph numbers 7895 and 7896).

The information gained from these sources showed that the source area and the proximal part of the depositional area still maintained their original shapes in April. Some small debris in the source area, however, had been washed out by rain, so that patches of the sliding surface showed in April.

Details of the original landforms and other features of the slide area were obtained from interviews and aerial photographs with a scale of 1:10,000, which were taken by the Geographical Survey Institute in 1977.

The Shimoda Forestry Office made a survey map of the slide area with the scale of 1:1,000 within two weeks of the landslide. I have added contours at 2-meter intervals from simple measurements made with an altimeter and pocket compass. This map was used as the base map for my study of the landslide.

Four hand auger borings were drilled through the sliding surface in the source area in May 1978. The paleosol was sampled in June to check its textures. Its mineral composition was determined by X-ray analysis, and a direct shear test was performed on it at the site in June. Six other landslide and nonslide areas also were surveyed briefly.

2.2 Description of the Landslide

2.2.1 *The original landform*

The landslide at Nanamawari occurred on a triangular slope with a 150-m base, a 150-m slope length and an average inclination of 25° toward the southeast (Figs. 2 and 3).

Before the slide, the slope was traversed diagonally by a path about 2 m wide and about 5 m deep at maximum, running northeast to southwest. The cut depth of this path decreased northeastward. The lower, southern part of this slope also was cut by a small but steep stream wall tranding N–S. The stream originated from a spring on the lower part of the slope just below the path; it was steep on the west side, but gradually changed to a gentle slope then a flat surface at the eastern side of the foot of the slope.

At the foot of the slope, a fluvial deposit with flat top surface cut from north to south by the Tajiri River was present. This had a westward facing slope on its east side.

Trees on the slope (the slide source area) were mainly conifers above the path with orange and broad-leaf trees below it. There were nine houses, rice fields and orange orchards on the flat surface at the foot of the slope. The slope was almost smooth and showed no landslide topography just before the earthquake.

2.2.2 *Post-slide conditions*

The path that traversed the slope before the slide remained as a "terrace" afterwards. The small stream wall also remained as a steep wall although its southern part was buried under debris (Figs. 2 and 3).

The landslide area is divided into the source and depositional areas. The source area has two parts, the triangular slope above the terrace (source area A in Figs. 2 and 3) and the trapezoidal slope below the terrace and to the west of the stream wall (source area B in Figs. 2 and 3).

Source area A is bounded on its upper side by a nonslide area with a nearly vertical cliff about 3 m high. A similar cliff forms the boundary between source area B and the nonslide area to its west.

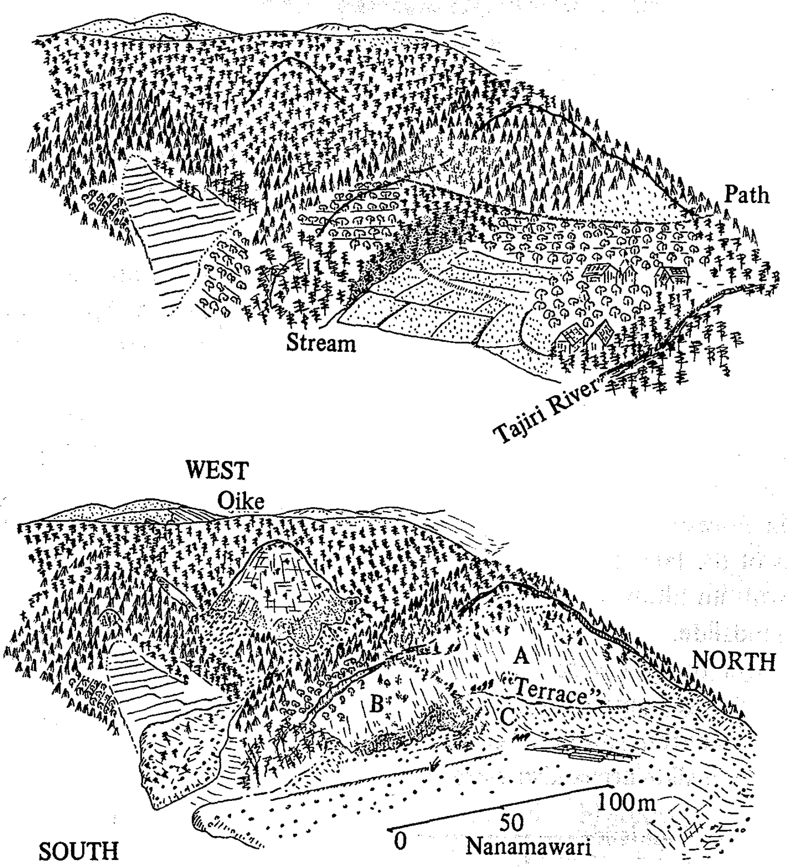

Fig. 2 Sketch of the landslide at Nanamawari: before (upper) and after (lower) the landslide.

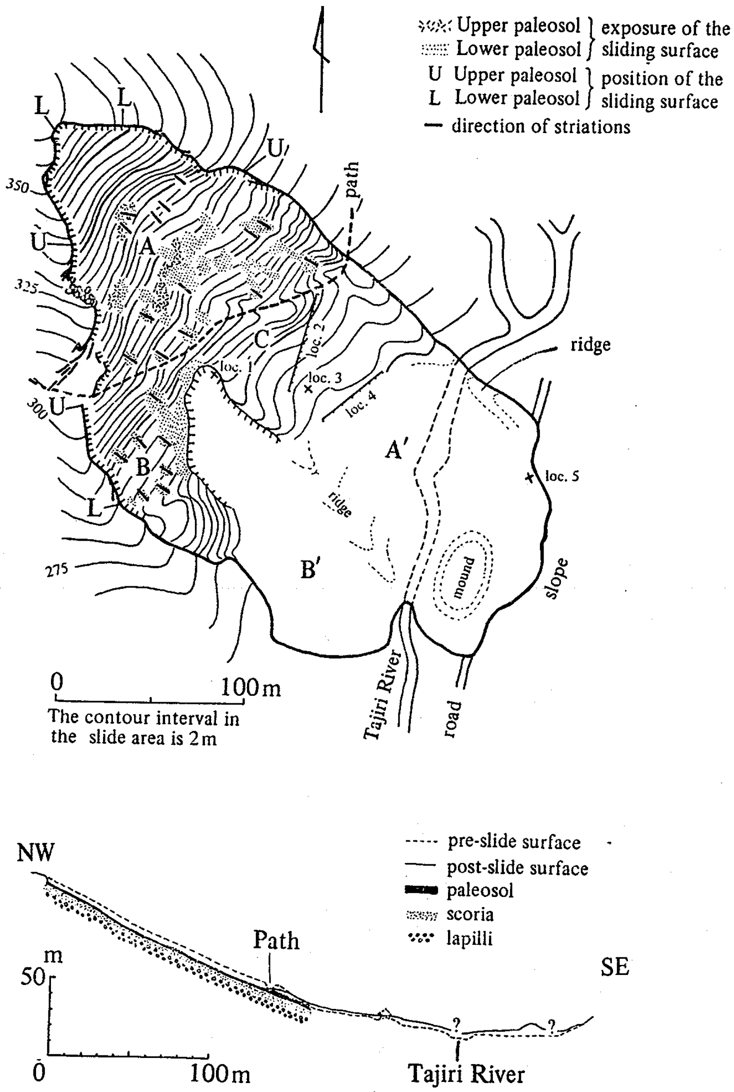

Fig. 3 Detailed map of the landslide at Nanamawari and its profile. Locality numbers (loc. 1–5) show the points where the internal structures of the beds or debris were observed (see text).

A depositional lobe-shaped area covers the slope below the terrace, the slope east of the stream (slope C in Figs. 2 and 3), the stream bottom, the flat top surface of the fluvial deposits on both sides of the Tajiri River and the slope to the east of that river (Fig. 3). Part of this depositional area is on a slope below source area B where sliding debris was deposited as a small mound.

Photographs taken of excavations in the depositional area immediately after the landslide show clear cross sections of the deposits at the proximal and distal ends of the depositional area.

The area of the landslide area was 47,800 m^2; 16,500 m^2 in the source area and 31,300 m^2 in the depositional area. The material that slid from the source area is assumed to have been 300–350 cm thick (2.2.3) with a calculated volume of 49,500–57,750 m_3.

2.2.3 *Geology*

Beds in the source area are composed of pyroclastic fall deposits with stratification dipping about 25°, from the surface of the slope. The succession was determined from observations of outcrops at the stream wall, at the sliding surface and at the small cliff bounding the source area. Data from hand auger borings and the exposure made along the crosscut in the source area in 1979 augmented visual observations (see Fig. 11).

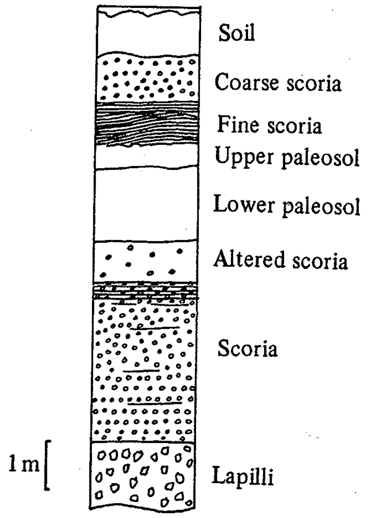

Fig. 4 Schematic columnar section of the pyroclastic fall deposits at Nanamawari.

The succession of the beds in ascending order is lapilli (more than 1 m thick), scoria (3 m 40 cm), altered scoria (80 cm), paleosol (1 m 20 cm to 2 m), fine scoria (60 cm to 1 m), coarse scoria (1 m), and soil (60 cm to 1 m) (Fig. 4).

The sliding surface formed in the paleosol [4] and this caused the 300 to 350 cm thick layers above it to slide. Part of the paleosol and the layers above it show as an outcrop at the cliff that surrounds the source area. Part of the paleosol and its underlying strata show as an outcrop at the stream wall.

(1) Beds that slid

The paleosol is sticky and very weak, being easily penetrated by a pencil. Many small holes, about 1 mm in diameter penetrate it. These probably are traces of the dissolved roots of plants. The paleosol is divided in two by differences in color; the light-brown section is the upper paleosol and the brown section the lower paleosol. These two parts gradually merge. The characters of the paleosol are described in detail in section 2.4.

The fine scoria bed above the paleosol is composed of black or reddish brown scoria grains 1 mm or more in diameter and has laminae of these grains. It tends to separate along the bedding plane and disintegrated into the constituent grains when scraped with a knife.

The coarse scoria bed above the fine scoria is composed of scoria grains a few millimeters to one centimeter in diameter. These grains are black or reddish brown internally with surfaces altered to yellow. The grains are weakly bonded and are easily separated by hand.

The soil is black in the upper 10–30 cm, but brown below. Plant roots are present within this soil, but do not reach the coarse scoria bed beneath it.

The boundaries between the paleosol and the fine scoria above it, as well as between the fine scoria and the coarse scoria above it, are clear and wavy. The boundary between the paleosol and the altered scoria beneath it is clear and smooth in some parts, but gradual in other places.

(2) Strata lower than the paleosol

The altered scoria bed is composed of scoria and brown clay, and is breakable with a pick. This bed contains plant fragments 3 cm thick and 20 cm long at the maximum. These fragments have a radiometric age of $40,400 \pm 1400$ B.P. (TK-239).

The scoria beneath the altered scoria bed is composed mainly of scoria grains with subordinate lapilli and blocks. Its black or reddish brown grains are several millimeters to 2 cm in diameter. They are well bonded to one another and are not easily separable by hand. At its top, the bed is in contact with the altered scoria and at its base with the lapilli bed, both along nearly smooth planes.

The lapilli bed beneath the scoria is composed mainly of lapilli with subordinate blocks; it outcrops at the lowermost part of the stream wall. It is from this bed that the stream springs.

(3) Trace of an old landslide

It is important to understand previous landslide history when investigating recent catastrophic landslides. Most of the surface materials on slope C (Figs. 2 and 3) did not slide in the 1978 landslide, but internal structures that indicated an old landslide were found at the head of the stream (loc. 1 in Fig. 3) and at the crosscut (loc. 2 in Fig. 3) trending NNE–SSW that had been made in slope C in October 1979.

At the head of the stream, the upper part of the fine scoria bed has collapsed and protrudes 70 cm intc the lower part of the coarse scoria bed above it at a right angle to the bedding plane (Fig. 5). The base of this fine scoria has not been disturbed; stratification is well preserved, as a whole. The paleosol, fine scoria and coarse scoria beds, as well as the soil are all layered in ascending order.

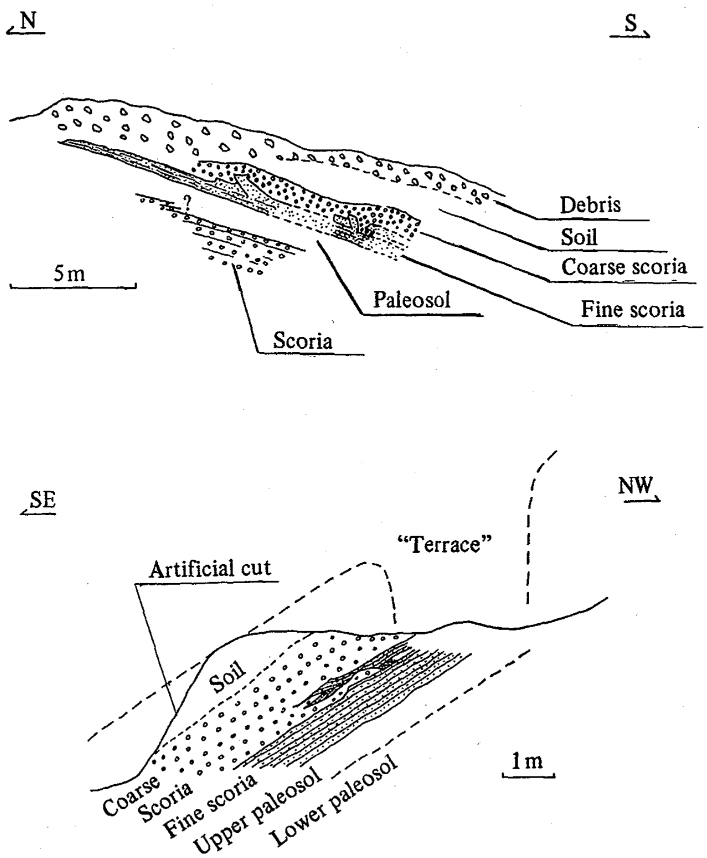

Fig. 5 Sketches showing the trace of an old landslide, (loc. 1 [upper] and loc. 2 [lower] shown in Fig. 3.). The upper part of the fine scoria bed protrudes into the lower part of the coarse scoria bed, but as a whole stratification is well preserved.

At the trench, the upper part of the fine scoria bed thrusts a thin layer, about 10 cm thick, into the lower part of the coarse scoria bed above it (Fig. 5). In contrast, the base of the fine scoria bed has not been disturbed. In general, stratification is well preserved.

Distortion of stratification is restricted to the upper part of the fine scoria and the lower part of the coarse scoria beds. It does not extend to the lower part of the fine scoria bed. This shows that the distortion was caused by the sliding of the upper part of the fine scoria, the coarse scoria and the soil, the sliding surface being within the fine scoria bed, not within the paleosol. The distorted part is tight with no open cracks; thus, the sliding shown by this distortion was not made during the recent earthquake; it is older.

The old landslide is presumed to have been of small scale in comparison with the 1978 landslide because its source area is nearly flat and shows no landslide topography. Layers, probably of uniform thickness, have slid from the old source area and the sliding surface formed within the paleosol beneath the fine scoria bed has outcropped after the recent landslide.

(4) Fault at the stream head

A fault was found at the stream head that cuts the paleosol and the beds beneath it. This fault, striking N 35°E and dipping 40°NE, appears to be a reverse fault with a 1-m displacement in its dip-slip component. There is no open crack along the fault plane. Therefore, no displacement seems to have occurred along this fault during the 1978 earthquake.

2.2.4 *Source area*

The source area is a triangular slope inclined southeastward. It is divided in two by a "terrace" (the trace of the path that existed before the slide) into a triangular source area, A, above the terrace and a trapezoidal source area, B, below it. Source area B is bounded by a steep stream wall on the east.

A nearly vertical cliff about 3 m high forms the boundary between source area A and the nonslide area. The cliff is V-shaped with the vertex at the top. This cliff is not easy to make out on the lower part of the slope because a large amount of debris hides it at the eastern margin of source area A and because many open cracks have formed near the southeastern margin of the same area.

These open cracks have formed where there were conifers, bush, or grass. Open cracks on the ground in the coniferous forest are found along the boundaries between the root systems of the conifers. They produce a honeycomb pattern with one or more trees in each cell. Open cracks in the area with bush or grass do not form a honeycomb pattern and tend to run NE–SW at right angles to the direction of the landslide.

A similar cliff is present between source area B and the nonslide area to its west. There are few open cracks in the nonslide areas around source areas A and B, except near the southeastern margin of A where there are many open cracks as described above.

The surfaces of source areas A and B are generally smooth because most of the materiasl in these areas have slid away. Only a small amount of debris remains.

(1) Soil layer blocks and debris

In the upper part and on the lateral sides of source area A, much debris, about 1 m or more thick, remains as well as many soil layer blocks that are limited by the root systems of one or more of the trees in them (Photo 2). Most trees in the blocks were standing and alive in June 1978. The debris is especially thick along the lower northeastern side.

Photo 2 Soil layer blocks and debris remaining in the upper part of source area A in Fig. 4.

In the middle of the lower part of A, however, the debris is only a few or several tens of centimeters thick, and the soil layer blocks are scattered. Some debris and soil layer blocks are trapped on the terrace. In source area B several soil layer blocks and debris, 1 meter or less thick, remain.

The debris in these two source areas is composed of disaggregated scoria (particularly coarse scoria), soil, paleosol, and blocks with a maximum diameter of about one and a half meters (Photo 2). Most blocks are composed of fine scoria, coarse scoria, or both. A few are made up of coarse scoria, fine scoria, and paleosol. The blocks, many with diameters of more than 1 m, are larger than those in the depositional area.

(2) Sliding surface

Some researchers say that the landslide was caused by the liquefaction of scoria. The following facts prove, however, that sliding took place on a sliding surface produced within the paleosol bed:

1. A sliding surface, slickensided on the paleosol with many groove-like striations, was found in patches of outcrops in the source area because a considerable amount of the fine surface debris had been washed away by rain after the landslide (Fig. 3 and Photo 3).
2. Undisturbed paleosol was found beneath the debris at six points along the foot of the cliff around source areas A and B (Fig. 3). At one point, on the uppermost part of source area A, undisturbed paleosol is present beneath the debris at a place where the moving debris probably had not considerably hollowed the paleosol.
3. The landslide debris is composed only of the paleosol and materials from the beds above it.
4. Some blocks of debris contain paleosol material as well as scorias.

Photo 3 Sliding surface with groove-like striations in the paleosol.

(3) Lateral support by the lower part of the slope

To investigate the causes and mechanism of the 1978 landslide, we needed to know whether the beds that slid had had lateral support before the slide. A clue was provided by the fresh plants roots present in the lowest part of the source area slope after the slide.

The cliff around the source area showed that plant roots are limited in the soil, and even at their lowest points, do not reach the coasre scoria bed beneath it. Thus, we concluded that the plant roots in this area did not originally penetrate the soil, coarse scoria, and fine scoria to what was to become the sliding surface.

After the landslide, however, fresh plant roots were seen penetrating the sliding surface along the terrace trace of the path. Given these observations, part of the paleosol must have been exposed along the path before the slide. Thus, part of the paleosol, and consequently the beds above it in source area A, must have been cut by the path and therefore did not have lateral support from the strata on the lower slope before the landslide. This inference matches the fact that the path had a depth of about 5 m at the maximum and that the sliding surface at this time was about three and a half meters below the original surface of the slope.

Before the landslide, a similar condition must have been present along the stream wall that bounds most of the lowest part of the slope of source area B. Afterwards the sliding part of the paleosol and the beds beneath it showed up as outcrops along the stream wall. These beds are gently inclined and cut by the stream wall. They also have fresh plant roots and lichens in patches along the stream wall surface. This shows that the outline of the stream wall, itself, was not much changed by the sliding. Consequently, the beds must have been cut by the stream wall before the 1978 landslide.

The stream wall formed the lower margin of the northeastern part of the slope of source area B (three-fourths of source area B); accordingly, the surface beds in this part probably were not supported laterally by the strata on the lower slope before the slide. In the southwestern part (one-fourth of area B), the slope continued smoothly downward as it had not been cut by the stream wall before the landslide.

2.2.5 *Depositional area*

(1) Morphology

The depositional area is lobe-shaped, except for a small mound of deposits on the slope at a point lower than source area B. These lobe-shaped deposits cover slope C, the small stream bottom, the flat surface at the foot of the slope, the Tajiri River, and the flat surface and slope on the opposite side of that river.

Two ridges of debris several meters high, trending NW–SE, are present along the northeastern margin and in the center of the depositional area, where there were no ridges before the slide (Fig. 3). The depositional area is divided in two, the northeastern (A′ in Fig. 3) and southwestern (B′ in Fig. 3) parts, by the ridge in the center of the depositional area.

Northeastern part: *A′* The northeastern depositional area, A′, is lobe-shaped with two lateral ridges along its northeastern and southwestern margins. Its southeastern margin is along the road running from its north to its south on the slope east of the road in the middle of the margin. The top of the margin on the slope is about 8 m above the road and is about 15 m above the Tajiri River.

A mound of deposits about 8 m high and 50 m in diameter, is located between the road and the river above the surrounding deposit surface (Fig. 3 and Photo 4). The center of this mound is about 30 m SSW from the centerline of A′, trending NW–SE.

The deposits show a rather smooth top surface except for the lateral ridges and the mound in the southeast. The deposits in the lateral ridges are at least 4 m thick, and in the northwestern part of slope C and its neighboring flat surface a few tens of centimeters to about one meter thick. The deposits average about 10 m in the mound in the southeast of A′; elsewhere the average is several meters thick, as judged from photographs taken after the landslide.

Southwestern part: *B′* The southwestern depositional area, B′, covers the stream bottom, the flat plane to the southeast of it and the slope at points lower than source area B. It does not reach the Tajiri River.

Although the complete morphology of the deposits in B′ is not clear because of scarcity of data, the deposit on the stream bottom is at least 3 m to 4 m 60 cm thick [5] and has a smooth

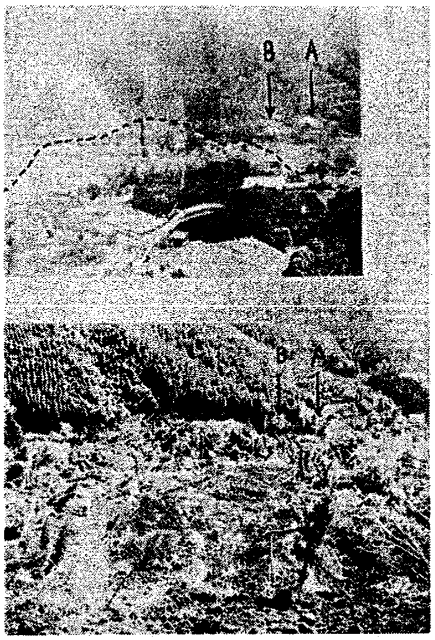

Photo 4 Oblique view of depositional area A′, looking southeast, before the slide (upper), and on the day after the land slide (lower). A and B in the photographs represent constructions that were not damaged by the landslide. Photographs courtesy of Mr. K. Tsuchiya (upper) and the Shimoda Police Station (lower).

top surface. Along the slope below source area B, the deposits form a mound five to six meters high above the sliding surface in B, so the over-all deposit on B′ is probably a few meters thick. Deposits were found among orange trees that were not dislodged from their pre-landslide position along the southern margin of the mound.

(2) Debris

Internal structures and the composition of the debris, observable in the northeastern part (A′) of the depositional area are described northwest to southeast from the source area. Debris in the southwestern part (B′) probably is similar to that in A′, but it was not observable.

Proximal part: slope C and its neighboring flat surface Along slope C, the site of an orange grove before the slide, little surface materials were moved, but the orange tree roots and surface soil were eroded. Soil with some plant roots remains covered by debris a few tens of centimeters to 1 m thick along the upper part of this slope. Along the lower part (loc. 3 in Fig. 3), an orange tree with its roots in soil had been flattened to the southeast, but not dislodged. It is covered by debris 1 m thick.

Debris on slope C and its neighboring flat surface is composed of disaggregated scoria grains (especially coarse scoria grains), soil, blocks of scoria 1 m across at maximum, and clods of paleosol several tens of centimeters thick and a few meters wide. Many of the blocks are composed of fine scoria. Blocks composed of coarse scoria, or of coarse and fine scorias, are few. The paleosol clods make many small mounds a few meters in diameter (Photo 5).

Internal structures of deposits in the proximal part were checked at the northeast-trending vertical cross section of the deposits on the flat surface near slope C (loc. 4 in Fig. 3). This location is shown in Photo 6 and in the sketch, Fig. 6. At first glance, the deposit looked chaotic, but close investigation showed that it is layered. A layer about 1 m thick, composed mainly of black soil, forms the bottom part of the deposit. It is overlain by a layer composed mainly of paleosol clods which, in turn, is covered by disaggregated coarse scoria grains and fine scoria fragments several to several tens of centimeters across.

Photo 5 Small mounds of paleosol clods at the proximal part of depositional area A′, June 1978. Grass grew after the slide.

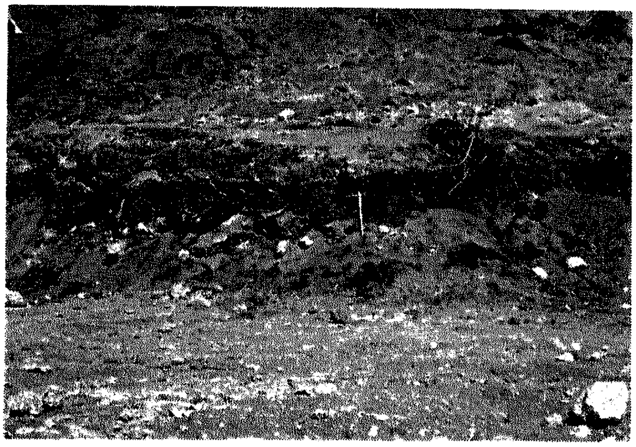

Photo 6 Photograph of the cross section of the deposits at the proximal part of depositional area A′ (loc. 4 in Fig. 4).

The black soil at the bottom generally is a few centimeters, or more, thick, although it thins out in places. It includes coarse scoria grains and fragments of fine scoria several millimeters to 2 cm across; thus, this black soil is allochthonous. The paleosol on it is separated into clods, several tens of centimeters thick and irregular outlines a few meters wide. The clods have some black soil near their bases, and fine scoria fragments, several centimeters to 30 cm across, and coarse scoria grains are present locally in them. The black soil and scorias in the paleosol clods probably were present when the paleosol clods slid.

Spaces between the paleosol clods are filled with black soil, coarse scoria grains, fragments of fine scoria, and small fragments of the paleosol. These space-filling materials are apt to be rich in black soil in the lower parts and rich in scorias in the upper parts.

Beneath the debris there is a homogeneous brown soil that has fresh plant roots. It is overlain by debris with a clear, smooth surface. Some peices of straw and vinyl, not heavily sheared, are sandwiched between the two locally. Grass had grown in the upper part of the soil in April 1978. These observations are evidence that the brown soil was the surface soil before the slide and that it was not hollowed deeply and differentially by moving debris.

Middle part Debris in the middle part of A′ was excavated just after the landslide. Judged from photographs (Photo 4, and others), the deposits were the same as in the proximal part, but many of the scoria blocks seem to have been less than several tens of centimeters in diameter.

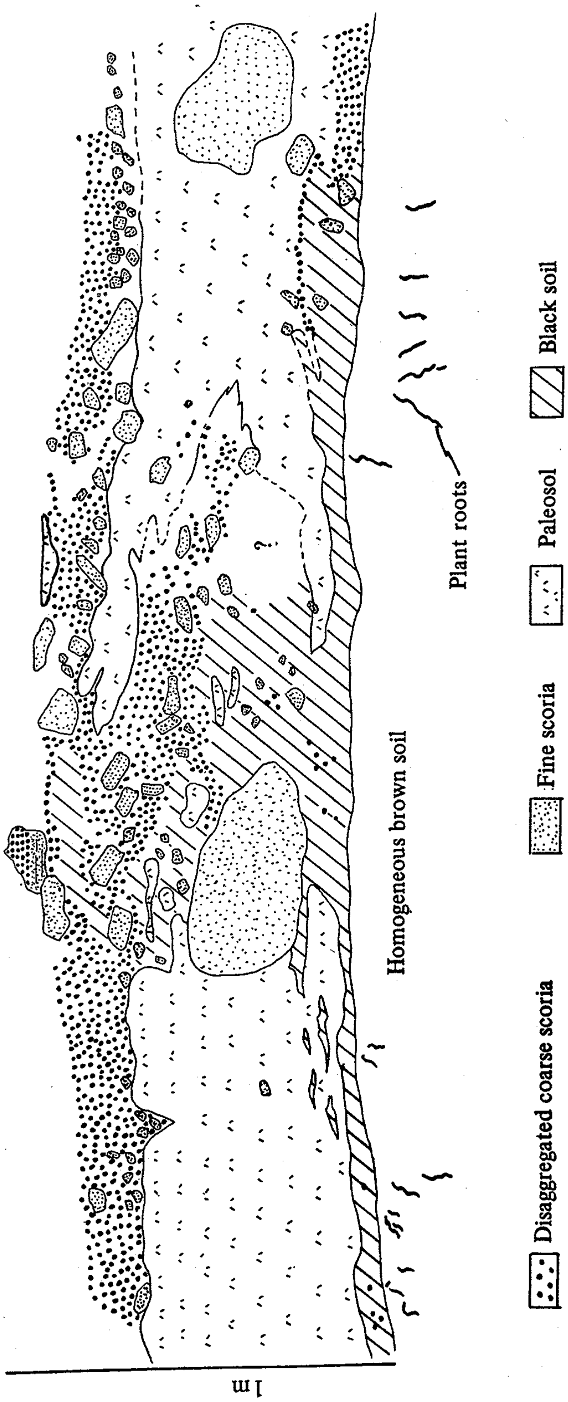

Fig. 6 Sketch of the internal structures of deposits at the proximal part of depositional area A′ (loc. 4 in Fig. 3). The cross section is perpendicular to the direction in which the debris moved.

Distal part A cross section of the deposits in the distal part was found along the road trending N–S (loc. 5 in Fig. 3). Photo 7, taken January 17th, shows a stratified deposit whose upper part is composed of brown material and whose lower part is composed of pale yellow material. The color of the yellow material indicates that it probably is rich in coarse scoria, and the part with brown material probably is rich in soil.

In April 1978, I observed the yellow colored deposit at the point shown in Photo 7. The parts of this deposit were made up of irregularly alternated beds of disaggregated coarse scoria grains and soil (Photo 8), each bed being several centimeters thick. These alternated beds must have been formed by the landslide because there are no beds like this in the cliff abutting the source area and because the constituent materials of the beds are disaggregated scoria and soil.

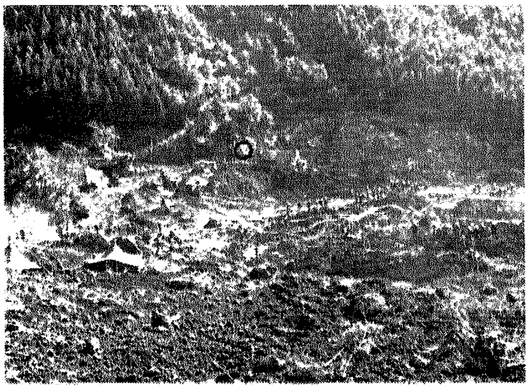

Photo 7 Photograph of depositional area A′ during its excavation, looking southeast. The crosscut of the deposits at the distal rim is at the top of the photograph. The circle indicates the area shown in Photograph 8. Photograph courtesy of the Shimoda Police Station.

Photo 8 Alternating beds of disaggregated coarse scoria grains and soil in the deposits at the distal part of depositional area A′. This area is shown in Photograph 7 as an open circle. It is loc. 5 in Fig. 4.

Photo 7 shows that the deposit in the distal area has no large blocks, but I found paleosol clods 10 cm thick and 1 m wide as well as fine scoria fragments less than 10 cm across in deposits disturbed by excavation.

2.2.6 *Transportation of plants and houses*

Most plants that grew on the source area before the slide were moved without much mixing up with the debris; they were located on the top of the deposits. The distribution of plants in the landslide area before and after the landslide is shown in Fig. 7. Trees on the slope along the southeastern margin of depositional area A″ before the slide were carried SE to SSE by moving debris, but not dislodged (see Photo 7).

The nine houses located on the depositional area before the slide were crushed completely by the moving debris and were found in the lower part of the deposits after the landslide. The fragments of these houses were not scattered, parts of each house being found in a mass (oral communications from officers of the Shimoda Police Station). Transportation of these houses is shown in Fig. 7.

Five of the seven victims were found with the houses; the other two bodies were found at a work site about 30 m southwest of the house in the center of A′ on the right bank of the Tajiri River. These two people, who probably had been working during the earthquake, are believed to have been buried (but not dislodged) by moving debris.

2.2.7 *Estimation of the duration of the landslide*

Mr. Z. Tsuchiya (from whose house the landslide area is visible) told me, "When I went out of my house, feeling afraid of the shaking of the earthquake, the landslide had already finished." In addition, Mr. K. Tsuchiya and his wife, who live in a house 500 m southeast of the slide area and who re-enacted what they did during the earthquake, told me that violent shaking took place for about 30 seconds. Thus, the landslide started and finished in less than 30 seconds from the beginning of the earthquake.

2.2.8 *Precipitation conditions before the slide*

Precipitation conditions at the slide area were almost the same as those at the nearby station, Inatori, 3 km ESE of the site. Precipitation data for Inatori are given on a daily basis (Fig. 8) from December 1977 to January 1978 [6, 7]. There were two peaks of precipitation before the slide. One, a 74-mm fall in the middle of December, and the other, an 84-mm fall over three

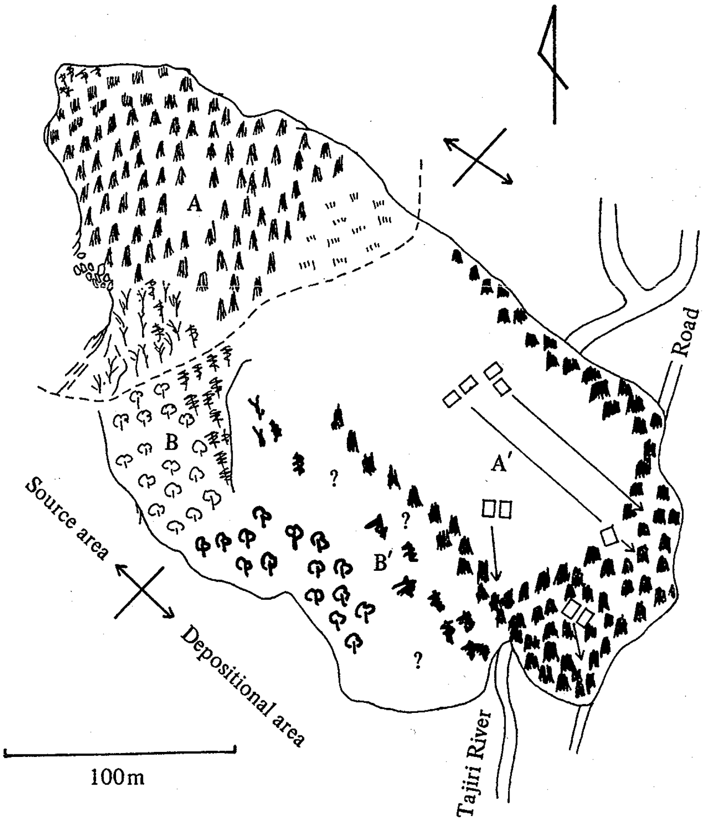

Fig. 7 Distribution of plants and houses before and after the 1978 Nanamawari landslide. Plants present before the sliding in the source areas (A and B) are drawn with fine lines, and those present in the depositional areas (A′ and B′) after the slide are drawn with heavy lines.

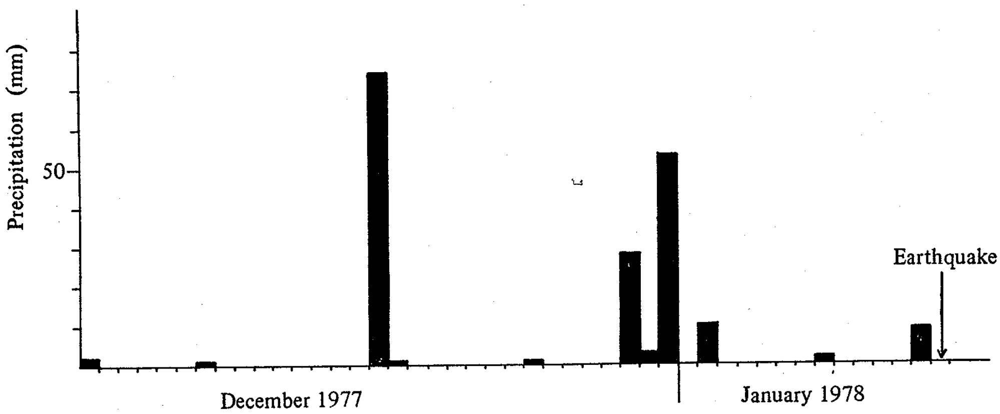

Fig. 8 Daily precipitation data, Inatori, December 1977 to January 1978 [6, 7].

days at the end of December. There was little precipitation during the 13 days that preceded the landslide.

The scorias and soil in the displaced materials are very porous and are permeable. In addition, the deposits immediately after the slide were dry and loose, shifting and compacting underfoot (oral communication from officers of the Shimoda Police Station). Therefore the scorias and soil in the displaced materials must have been dry at the time of sliding, but the paleosol beneath them presumably was not dry because it retains water well.

A dust cloud was seen in the direction of Nanamawari during the earthquake at Mitakahama about 3 km southeast of there. It is believed to have been generated by the landslide and probably shows the dryness of the displaced materials.

2.3 Reconstruction of Landslide Phenomena

Landslide phenomena are classified based on the descriptions given in section 2.2.

2.3.1 *Modes of movement*

Slide and debris flow are indicated as the modes of movement for the displaced materials, but most materials that slid were dry. Although these two modes may be called a debris avalanche, the term avalanche does not indicate the modes of movement; therefore, I have not used it in this paper.

(1) The slide

Striations in the sliding surface show that sliding occurred. What was this sliding?

There are many paleosol clods a few meters in diameter that are detached from each other, in the proximal part of the depositional area (2.2.5). In contrast, many soil layer blocks remain in the upper part of the source area although they are scattered in its lower portion (2.2.4).

These phenomena show that the beds above the sliding surface did not slide as a slab, but as many blocks a few meters wide. Most soil layer blocks left in the upper part of the source area do not have coarse scoria, fine scoria and part of the paleosol regularly located beneath them; a thin layer of debris is present between them and the sliding surface. Accordingly, except for the soil layers, the beds themselves must have disintegrated when they split into blocks. This splitting and disintegration of the beds are considered essential to the formation of the debris described later.

The splitting of beds into blocks and the sliding of these blocks probably began along the lower margin of the source area, the cut of the path and the stream wall, immediately developing upward retrogressively (Fig. 9).

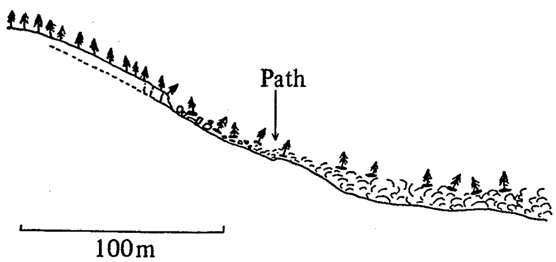

Fig. 9 Schematic sketch of the modes of movement: slide and dry debris flow.

In the lower southwestern part of source area B, the beds presumably had not been cut before the slide (2.2.4). They are believed to have been induced to move by the sliding of beds to the east.

The retention of many soil layer blocks and debris in the upper part of the source area as compared to the lower part is explained as follows: By the time the splitting and sliding of the blocks had reached the upper part of the source area, the seismic tremor had decreased and was too weak to engender further severe sliding.

The splitting of beds and the retrogressive development of a landslide also were observed during the 1964 Alaska earthquake [8]. These two phenomena may represent the way landslides take place when triggered by earthquake [9].

(2) Dry debris flow

Dry debris flow of the moving materials is thought to have occurred because the size of the blocks of scorias decreases from the source area through the proximal part to the distal portion of the depositional area. In the distal part, some debris shows stratification of alternated beds of disaggregated coarse scoria grains and soil; whereas, elsewhere the debris is made up of a generally chaotic mixture of soil, fine scoria, coarse scoria, and paleosol. The debris did not hollow the surface soil beneath it deeply or differentially. The debris was dry and loose immediately after the slide which generated a large dust cloud. The phenomena cited here are described in sections, 2.2.4, 2.2.5, and 2.2.8.

Cumulative evidence shows that the constituent materials were considerably disintegrated by the splitting of beds, continued to disintegrate during movement, and flowed in a dry condition into the depositional area (Fig. 9). The direction of movement (given later) also indicates that the debris did flow. The abundance of paleosol clods in the proximal part of the depositional area presumably means that the flowing debris was composed mainly of fine scoria, coarse scoria and soil.

Soil layer blocks with one or more trees in their centers probably floated on the flowing debris because the blocks were not mixed much with the debris and were found on top of the deposits after the landslide.

The splitting of the beds accompanied by their disintegration is considered to have been a necessary precursor to the formation of the debris. If beds had slid as unsplit slabs, no flow of debris could have formed.

The dry debris flow described for this landslide resembles that of rock and snow avalanches. And, although there are several hypotheses for the mechanism of avalanche movement [3, 10, 11, 12, 13, 14], dry debris flow and rock avalanches need further study, especially many more field examinations and experiments.

2.3.2 *Direction of movement*

As described in section 2.2.6, plants originally in the main part of source area A moved southeastward, the dip direction of the slope, and settled in depositional area A′, whereas plants from B and the southwestern part of A moved southeastward and settled in B′.

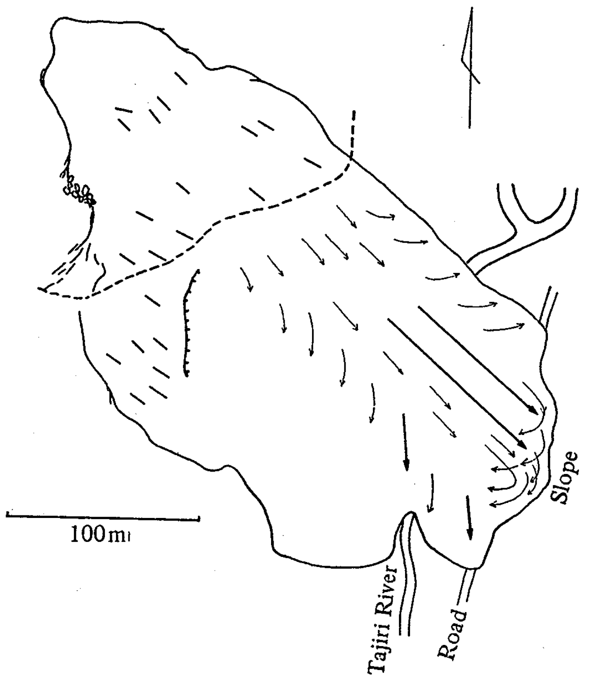

Fig. 10 Schematic sketch showing the direction of them ovement of the sliding material. Short lines show the direction of striations. Thick arrows show the displacement of houses. Thin arrows represent the presumed direction of debris movement.

The direction of the movement of materials from source area A was determined from the following phenomena (see sections 2.2.4 and 2.2.6). Conifers from A are distributed densely in a U-shaped zone with its convex side to the southeast in depositional area A′, the two straight parts of the "U" corresponding to the two lateral ridges of the deposit. These conifers, thus, are distributed mainly along the rim of the deposits in area A′. The four houses in the south of A′ were transported toward the SSE to the lateral ridge made by the landslide, whereas the four houses in the center of A″ were transported southeastward.

This means that the center of the debris flow moved southeastward along the center line of A′, and that its side parts moved toward the SSE or ENE, away from the center line of A′ (Fig. 10).

At the distal part of depositional area A′, the highest point of the deposit on the westward facing slope is on the center line trending NW–SE of depositional area A′. In contrast, the center of the distal mound of the deposit is on the flat surface 40 m southwest of the highest deposit point on the slope. Plants that grew on the slope before the slide were carried down toward the SSW to SSE by the moving debris, but were not dislodged. This is evidence that the center of the debris flow rushed southeastward, dashed against the westward-facing slope, then rebounded southwestward to form the mound of debris on the flat surface (Fig. 10).

2.3.3 *Velocity estimation*

The distance from the top of source area A to the southeastern rim of depositional area A′ is about 350 m. If the materials moved this 350-m distance in 30 seconds (2.2.7), their velocity would average 11.7 m/sec (42 km/h). The maximum velocity, however, was probably greater because the duration of the landslide may have been less than 30 seconds and because the velocity of the material changed from zero through the maximum to zero again.

2.4 The Paleosol in which the Sliding Surface Formed

2.4.1 *Position of the sliding surface*

The position of the sliding surface in the paleosol bed was determined from outcrops of the sliding surface, hand auger boring data, and a crosscut made in the source area in October 1979 (see Fig. 11).

The paleosol bed is divided in two parts by differences in color; light brown marking the upper paleosol and dark brown the lower paleosol (2.2.3). The paleosol bed appears to be 130–230 cm thick and the upper paleosol about 40 cm thick, measured vertically. The true thicknesses of these beds are apparent thicknesses multiplied by cos 25° (0.91) as the beds are inclined about 25°.

The sliding surface is located in the paleosol above a point 70 cm from its base, most of the sliding surface being in the lower paleosol, with a small amount in the upper paleosol (Fig. 11). Consequently, the sliding surface in the upper part of the lower paleosol covers a large area. The reason for the sliding surface being formed in a restricted zone was determined by mineralogical investigation.

2.4.2 *Mineralogy*

The mineral composition of the paleosol was checked by X-ray analysis. The vertical distribution of its mineral components was determined at two points (a and b in Fig. 11). Results are shown graphically in Fig. 12.

X-ray analysis data for the paleosol at the point at which the sliding surface is in the upper paleosol is shown in Fig. 12a. The upper paleosol beneath the sliding surface has an apparent vertical thickness of 25 cm, and the lower paleosol 105 cm. The lower part of the lower paleosol within 70 cm of its base is rich in gibbsite with halloysite or a 14 Å clay mineral scarcely as secondary minerals. Both the upper part of the lower paleosol and the upper paleosol, more than 70 cm from its base, are rich in halloysite with a subordinate 14 Å clay mineral and gibbsite rarely.

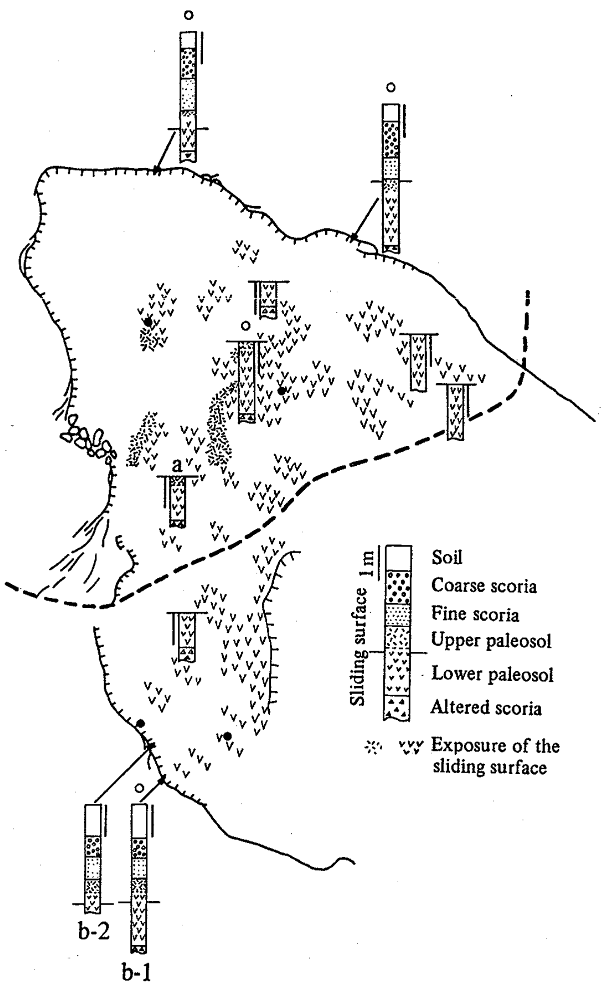

Fig. 11 Map showing the position of the sliding surface in the paleosol. Solid circles indicate the sampling points for direct shear tests. a and b (b–1, b–2) show the sampling points for systematic X-ray analysis. Columnar sections with open circles are based on boring data. The other columnar sections are based on exposures along the crosscut or cliff.

X-ray analysis data at the cliff bounding the source area where the sliding surface is in the upper part of the lower paleosol are shown in Fig. 12–b. The lower paleosol tends to be rich in gibbsite in its lower part and rich in halloysite with a subordinate 14 Å clay mineral in its upper part. The lower part of the upper paleosol shows only a distinct peak for quartz in its X-ray profile; it probably is composed mainly of amorphous materials. The upper part of the upper paleosol is rich in halloysite.

Samples of the paleosol taken just beneath the sliding surface at other five points were all rich in halloysite. One sample was from the upper paleosol, the other four from the lower paleosol.

Besides these minerals, quartz was present in all the samples with feldspar, opal, magnetite, and interstratified mica-montmorillonite sometimes was present. Clay minerals in the $<2\mu$ fraction were the same as those detected in the bulk sample.

The paleosol has mineralogical zonation as shown, the lower part of the lower paleosol tending to be rich in gibbsite and the upper part of the lower paleosol and the upper paleosol tending to be rich in halloysite (with limitted amorphous materials in the upper paleosol). The sliding

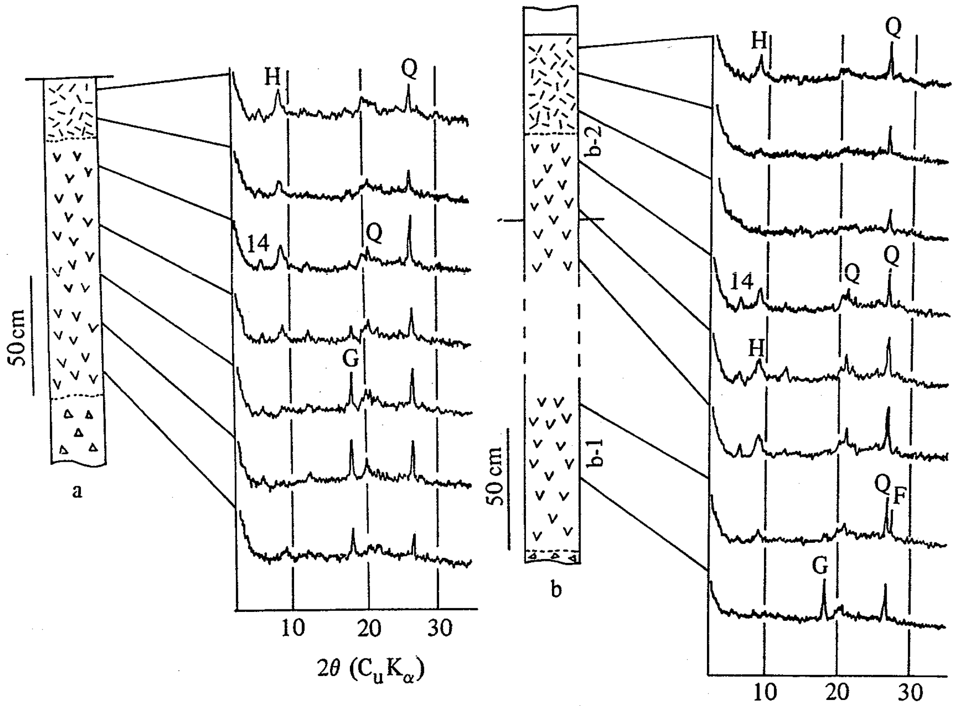

Fig. 12 Columnar sections of the paleosol and the correesponding X-ray diffraction diagrams. The legend and sampling points are given in Fig. 11. H, halloysite; 14, 14 Å clay mineral; G, gibbsite; Q, quartz; F, feldspar.

surface is located in the upper part of the lower paleosol and in the upper paleosol (2.4.2). The paleosol just beneath this sliding surface is rich in halloysite, evidence that the landslide is related to the mineral zonation of the paleosol and that the sliding surface was formed selectively in the halloysite-rich part.

Volcanic ash, or loam, is known to weather to halloysite, gibbsite, 14 Å clay minerals, and other minerals [15]. The zonation of the halloysite-rich and gibbsite-rich parts of the paleosol, however, has not been previously reported. This compositional zonation also is found in the paleosol in a non-slide area. It is described in detail in Appendix B.

2.4.3 *Textures*

The paleosol sometimes contains grains, probably weathered scoria grains several millimeters to 1 cm in diameter. Most of the lower paleosol grains are very weak and are easily crushed by the fingers. Grains are relatively more abundant in the upper paleosol than in the lower paleosol, some in the upper paleosol are not crushable with the fingers but can be cut with a knife.

The paleosol has root holes, probably traces of dissolved plant roots that once penetrated it (Photo 9). Most of the root holes are less than 2 mm in diameter, but ones of about 1 cm are present in the upper paleosol. Some undissolved roots are also present in the paleosol.

Textures of the paleosol beneath the sliding surface were checked at seven points with SOFT-X-ray photographs. One photograph was made of an upper paleosol sample, the others made were all of the lower paleosol. Root holes are flattened and almost extinguished by the plastic deformation of the paleosol within several to 10 cm of the sliding surface. White lines, probably shear fractures, are sometimes present in the deformed paleosol (Photo 10).

Plastic deformation predominates only near the sliding surface, away from this surface root holes without plastic deformation or shear fractures remain. This means that the relative displacement between the sliding material and the stationary area beneath it mainly took place along the sliding surface; it did not extend away from the sliding surface and the nearby horizon.

Photo 9 Root holes in the paleosol. The arrow indicates an undissolved plant root.

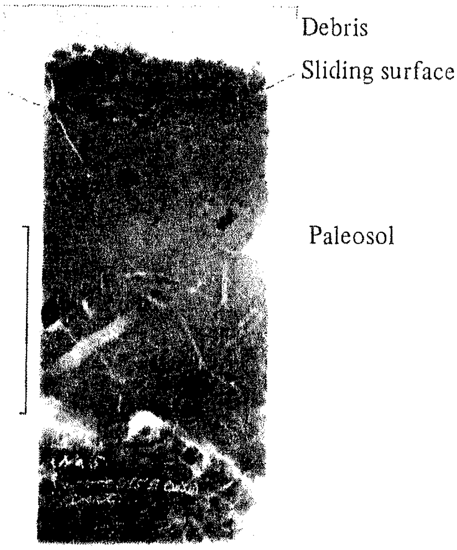

Photo 10 Textures of the paleosol beneath the sliding surface (SOFT-X-ray photograph). Root holes are flattened and almost extinguished by plastic deformation near the sliding surface.

2.4.4 *Shear strength*

The shear strength of the paleosol was measured at the site in June 1978 with a portable, direct shear apparatus (MARUTO, S07B).

(1) Sampling

The paleosol was sampled at three points, 10 cm to 30 cm below the sliding surface. The paleosol in the nonslide area was sampled at the lower part of the cliff that bounds source area B (Fig. 11). All the samples came from the halloysite-rich upper part of the lower paleosol. No shear tests were performed for the upper paleosol as it was difficult to obtain undisturbed specimens because of the hard grains present.

Each sample was cut with a trimmer to obtain undisturbed discoid specimens 20 mm thick and 50 mm in diameter. Two series of tests were made for the samples from each point; one a test in which the shear plane parallels the sliding surface, the other, one in which the shear plane is normal to the sliding surface. All tests were made under undrained conditions.

(2) Results

Results of the direct shear tests are shown graphically in Fig. 13. The shear strength values for each point are approximately linear in the τ–σ graph. The shear strength values for each point obtained from one test series are not much different from values obtained for the other, but the values of different points differ slightly. These value differences probably are due to differences in water content which must have differed at each point after the slide.

Thus, fracture line 1, determined by the method of least squares, is assumed to represent the shear strength of the halloysite-rich upper part of the lower paleosol.

$$\tau = c+\sigma \tan \phi_u \tag{1}$$

in which $c=0.24$ kgw/cm², $\phi_u=19°$, $R=0.89$, τ is shear stress, c is cohesion, σ is normal stress, ϕ_u is the internal friction angle, and R is the coefficient of correlation.

(3) Landslides and shear strength

Assuming that sliding occurs when shear fractures form in the paleosol, the horizontal acceleration of an earthquake sufficient to cause sliding could be calculated (see Appendix A for

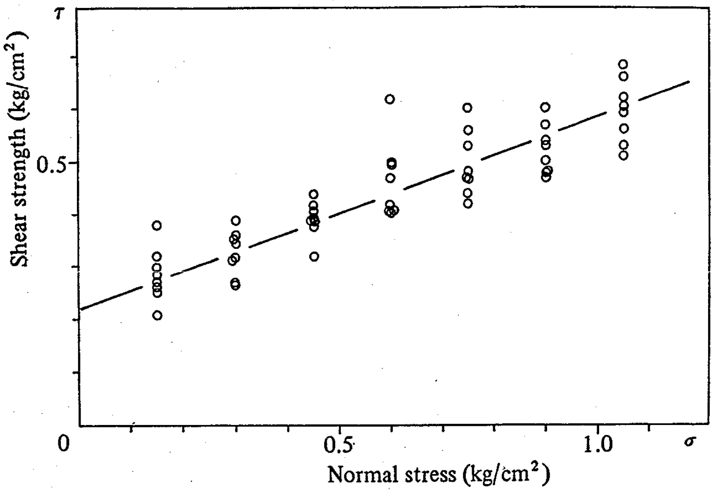

Fig. 13 Shear strength of the paleosol.

details). A horizontal acceleration of about 380 gals in addition to gravity would be sufficient to cause sliding. Some assumptions, however, were made before the calculations were done.

At Mitaka-iriya, the largest horizontal acceleration of the Izu-Oshima-Kinkai earthquake is believed to have been 400–450 gals, larger than the calculated 380 gals [16, 17]. Except for this case, the horizontal accelerations of earthquakes recorded after the early 18th century all seem to have been less than 380 gals [18]. The large acceleration value may explain why a landslide occurred in this earthquake but not in previous ones. Some points are still not clear, notably when the path and the stream wall cut the paleosol bed.

2.5 Causes of the Landslide

The causes of landslides can be divided into two groups; basic causes (conditions) favoring a landslide and initiating causes [19]. These two groups of causes are summarized here for the landslide at Nanamawari*.

(1) Basic causes

1. Surface materials were composed of Quaternary pyroclastic fall deposits that were stratified nearly parallel to the slope surface. This favored formation of a continuous smooth sliding surface.
2. A weak halloysite-rich paleosol was present several meters below the slope surface, and it was in this paleosol that the sliding surface formed.
3. Scorias and soil which were poorly bounded together predominated above the paleosol. These materials were favorable for the formation of the debris that flowed in a dry condition.
4. Most of the beds that slid had been cut by the path or the stream wall in the lower part of the slope. They therefore did not have sufficient support from the strata on the lower slope before the slide.

(2) Initiating causes

An earthquake tremor with a maximum horizontal acceleration of 400–450 gals was the initiating cause of the Nanamawari landslide.

* No evidence was found that a sliding surface or zone weakened by creep had been formed in the paleosol before the landslide caused by the 1978 earthquake. I therefore believe that there had been neither previous sliding nor creeping in this area. A sliding surface probably had formed in a slope steeper than this one (see section 3.2.1).

3. SIMILAR LANDSLIDES IN OTHER LOCATIONS IN MITAKA-IRIYA

3.1 General

Landslides similar to that at Nanamawari took place at six localities in Mitaka-iriya (II–VII in Fig. 1). In every one, all or most of the sliding surface was formed in the upper part of the paleosol several meters below the slope surface. Scoria, soil and part of the paleosol slid (Fig. 14). The scale of each landslide was about the same as, or less than, that at Nanamawari.

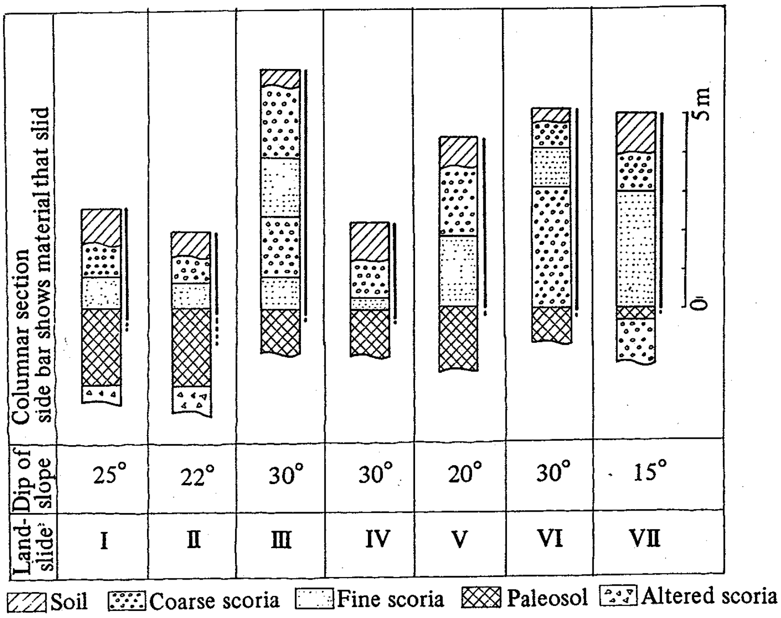

Fig. 14 Columnar sections and the dips of slopes in the seven landslide areas in Mitaka-iriya.

The source areas in these landslides were inclined 15° to 30° and were separated from the surrounding nonslide areas by small cliffs several meters high.

All deposits on the flat plane are lobate with lateral ridges and a distal mound on the plane. When a deposit buries the stream bed at a bend of the stream, the top of the deposit is higher on the under-cut slope than on the slip-off slope. Deposits are composed of disaggregated scoria grains, soil, paleosol, and blocks of scoria. Soil layer blocks with plant root systems lie on top of the deposits.

Halloysite was detected in the paleosols just beneath the sliding surfaces in four landslide areas (I, II, III, IV and VI). In the other two areas (V and VII), gibbsite was present. Halloysite, however, might be found on closer investigztion.

The morphologies of these six landslides and the materials that slid resemble those of the landslide at Nanamawari. This indicates that these landslides must have had the same mode of movement as at Nanamawari.

3.2 Why the landslides occurred locally

Landslides took place at only seven localities, but the same pyroclastic fall deposits seem to cover the whole of the neighboring area and would be the basic cause of the landslides. The factors that limited the number of landslides may have been the presence or absence of lateral support by the lower part of a slope and the relation between the direction of a slope and the direction of the earthquake tremor.

3.2.1 *Lateral support*

Conditions in the lower parts of source area slopes before the slides are considered. In landslides II, VI, and VII (Fig. 1) beds slid on a gentle slope above a knick line formed by stream erosion. These beds were stratified nearly parallel to the gentle slope. Probably, these beds that slid were cut by steep slopes lower than the knick lines and had no lateral support from strata in the lower parts of the slopes before the slides.

In landslide IV, the beds that slid probably had been cut by the road in the lower part of the slope before the slide. In landslide III, beds probably had crept and formed an overturned fold in the lower part of the slope before the slide, as in the collapse structure described by Harrison and Falcon [20]. Previous creeping in landslide III may be attributable to the fact that the beds that slid in this landslide were the steepest (30°) and thickest (6.4 m) of all those studied (Fig. 14).

In conclusion, it seems certain that landslides in Mitaka-iriya cocurred on slopes that had little lateral support from their lower part.

3.2.2 *Direction of the slope*

An examination of the direction of the slopes on which landslides took place showed that all seven landslides occurred on slopes inclined ENE to S (Fig. 1) even though there are many slopes inclined in other directions near the landslide areas. Thus, the occurrence of landslides also may be controlled by the direction of the earthquake tremors.

4. A COMPARISON WITH COLLAPSING LANDSLIDES OF PYROCLASTIC FALL DEPOSITS TRIGGERED BY OTHER EARTHQUAKES

Much of Japan is covered by young pyroclastic fall deposits. Many landslides similar to those at Mitaka-iriya took place during the 1968 Tokachi-Oki earthquake and the 1949 Imaichi earthquake (Fig. 15). These landslides were similar to those at Mitaka-iriya in their shifted materials, source morphology, depositional areas and rapid movement (Table 1). Their modes of movement, however, were not thoroughly determined.

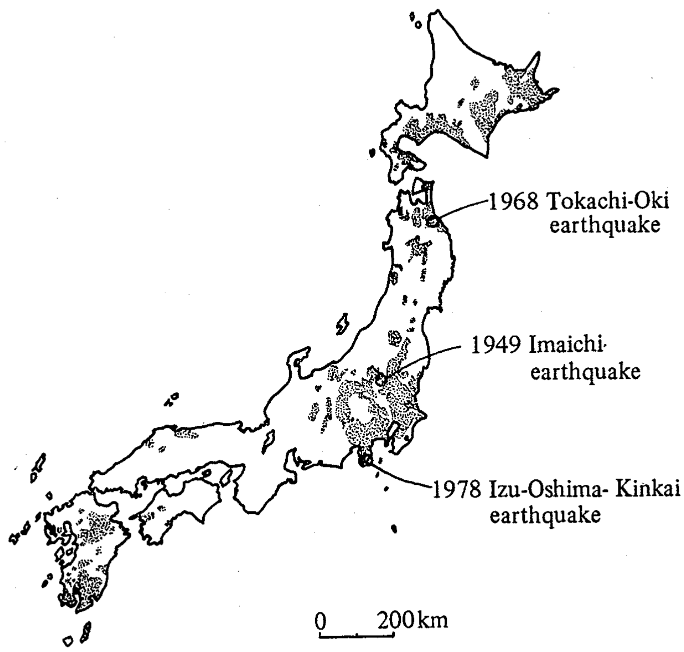

Fig. 15 Distribution of volcanic ash soils [15], and landslides similar to the one at Nanamawari.

Table 1 Comparison of landslides triggered by the 1978 Izu-Oshima-Kinkai, 1968 Tokachi-Oki, and 1949 Imaichi earthquakes.

Earthquake	The 1978 Izu-Oshima-Kinkai earthquake	The 1968 Tokachi-Oki earthquake	The 1949 Imaichi earthquake
Place	Mitaka-iriya (Nanamawari)	Hachinohe city	Noguchi in Nikko city
Materials that slid	Quaternary pyroclastic fall deposits (scoria, ash)	Quaternary pyroclastic fall deposits (pumice, ash)	Quaternary pyroclastic fall deposits (pumice, ash)
Sliding surface	upper part of paleosol rich in halloysite	boundary between ash and the pumice beneath it	halloysite-rich clayey layer
Deposits	lobe-shaped with lateral ridges, a distal mound on the flat plane soil layer blocks are on it dry	lobe-shaped and uniformly thick on the flat plane soil layer blocks are on it wet	lobe-shaped with a distal mound (lateral ridges ?) soil layer blocks are on it dry?
Duration	about 30 seconds	less than one minute	very short time?
References		(21)	(22, 23, 25)

4.1 1968 Off-Tokachi (Tokachi-Oki) Earthquake

Many landslides occurred in Hachinohe City and vicinity in Aomori Prefecture during this earthquake. Landslides composed of pyroclastic fall deposits, pumice and ash were particularly common. These depositional bodies cover exceptionally large areas as compared to their rather narrow source areas. The landslides took place in more than ten localities and caused many disasters. The sliding surface of all the landslides is believed to have been at the boundary between the ash and pumice just beneath the surface or nearby, several meters below the slope surface [21]. The mineral compositions near the sliding surface were not identified.

The Hachinohe landslides resemble those in Mitaka-iriya (Table 1), the only distinct difference between the two being the thickness of the deposits distributed on the flat surface and the dryness of the materials that slid. Deposits generally had uniform thickness in the landslides at Hachinohe, whereas they were thicker in the lateral and distal portions than in other parts of the deposits at Mitaka-iriya. The materials that slid were wet at Hachinohe, and dry at Mitaka-iriya.

At Hachinohe, the region in which landslides have been dense corresponds to the area in which 200 mm of precipitation had fallen in the three days preceding the slides [21]. Many reports mention that pumice or ash, saturated with water, was liquefied by the earthquake shock and caused catastrophic mudflows. But similar landslides took place under dry conditions at Mitaka-iriya. Therefore, although the precipitation that preceded the Tokachi-Oki earthquake might have been important in decreasing the shear strength of the zone in which the sliding surface formed, the water itself was not essential for the movement of these materials.

The thickness of the distribution of the deposits indicates that wet debris is less mobile than dry debris during its flow. The lesser mobility of the wet debris may be due to the surface tension of the unsaturated interstitial water.

4.2 1949 Imaichi Earthquake

Many landslides took place on slopes composed of Quaternary pyroclastic fall deposits of pumice and ash in and around the cities of Imaichi and Nikko in Tochigi Prefecture, during the 1949 earthquake. Some resemble the slides at Mitaka-iriya. The landslide at Noguchi in Nikko has been described in detail by Koide (Table 1) [22]. The sliding surfaces of these landslides are considered to have formed in a halloysite-rich clay layer several meters below the slope surface [23].

In addition, in the 1974 Izu-Hanto-Oki earthquake a sliding surface was formed in a halloysite-rich layer originating from Tertiary tuff. This tuff, tuffaceous sandstone, and volcanic breccia slid and flowed at Nakagi in the south of the Izu Peninsula [24]. Therefore, the presence of halloysite may be important in the formation of collapsing landslides of this type.

5. CONCLUSIONS

Collapsing landslides at Nanamawari, triggered by the 1978 Izu-Oshima-Kinkai earthquake, that were composed of pyroclastic fall deposits accompanied by dry debris flow, their phenomena and causes, were studied. The modes of movement at Nanamawari were shown to be very fast sliding and debris flow under dry conditions. The important basic causes of these landslides were insufficient lateral support by strata on the lower slope and a weak halloysite-rich paleosol in which the sliding surface formed.

Because Japan is covered widely by young pyroclastic fall deposits, landslides similar to that at Nanamawari have occurred during other earthquakes. Therefore the landslide at Nanamawari is considered typical of this type of landslide in Japan.

Several important questions remain unanswered: What is the mechanism of debris flow under dry conditions, the mechanical behaviour of halloysite-rich "soil" under dynamic shear, the origin of the zonation of the mineral composition of the paleosol and the behaviour of seismic waves in mountains. These questions must be answered by scientists expert in soil mechanics, geophysics, geology, and mineralogy.

ACKNOWLEDGEMENTS

This investigation was made under the guidance of Professor Toshio Kimura of the University of Tokyo, to whom I express my sincere gratitude for his instructive suggestions and criticisms of this manuscript. I also thank Associate Professor M. Utada, Drs. Y. Tsuneishi and T. Ito of the University of Tokyo and Dr. K. Kano of Shizuoka University for their critical discussions and encouragement both in the field and the loboratory.

The study was made possible by a grant from 1977 to 1979 from Science Research Funds for Natural Disaster Science (No. 202008, R. Morimoto representative), provided by the Ministry of Education, Science and Culture of Japan.

REFERENCES

[1] Japan Meteorological Agency, The Seismological Bulletin of the Japan Meteorological Agency, January 1978. (1978) [Japanese].

[2] Aramaki, S. and Hamuro, K., Geology of the Higashi-Izu monogenetic volcano group, Bull. Earthq. Res. Inst. Univ. Tokyo, Vol. 52, pp. 235–266 (1977) [Japanese].

[3] Heim, A., Bergsturtz und Menschenleben, Fretz and Wasmuth, Zurich, p. 218 (1932).

[4] Otsuka, K., Landslides near Nanamawari at Mitaka-iriya triggered by the 1978 Izu-Oshima-Kinkai earthquake —with special reference to geology and the sliding surfaces, In Report of a synthetic study of the disaster caused by the 1978 Izu-Oshima-Kinkai earthquake, pp. 37–38 (1978) [Japanese].

[5] Hatano, S. et al., Study of a landslide —in Mitaka-iriya and Nashimoto, In Sudo, K. and Hatano, S. eds., Earthquake Disasters in The Izu Peninsula, pp. 26–53 (1978) [Japanese].

[6] Japan Meteorological Agency, Monthly Report of Japan Meteorological Agency, January 1977. (1978) [Japanese].

[7] Japan Meteorological Agency, Monthly Report of Japan Meteorological Agency, December 1977. (1977) [Japanese].

[8] Hansen, W.R., Effects of the earthquake March 27, 1964 at Anchorage, Alaska, U.S. Geol. Survey Prof. Paper, 542A, p. 68 (1965).
[9] Seed, H.B., Landslides during eatrhquakes due to soil liquefaction, Am. Soc. Civ. Eng. Proc., Vol. 94, no. SM5. pp. 1055–1122 (1968).
[10] Kent, P.E., The transport mechanism of catastrophic rockfalls, J. Geol. Vol. 74, pp. 79–83 (1966).
[11] Shreve, R.L., Leakage and fluidization in air-layer lubricated avalanches, Geol. Soc. Am. Bull., Vol. 79, pp. 653–658 (1968).
[12] Bagnold, R.A., Experiments on a gravity-free dispersion of large solid spheres in a Newton fluid under shear, Proc. R. Soc. Lond., Ser. A, Vol. 225, pp. 49–63 (1954).
[13] Howard, K., Avalanche mode of motion: Implications from lunar examples, Science, Vol. 180, pp. 1052–1055 (1973).
[14] Hsu, K.J., Catastrophic debris streams (Sturzstroms) generated by rockfalls, Geol. Soc. Am. Bull., Vol. 86, pp. 129–140 (1975).
[15] Nagasawa, K., Weathering of volcanic ash and other pyroclastic materials, In Sudo, T. and Shimoda, S. eds., Clays and clay minerals in Japan, Developments in Sedimentology, Vol. 26, pp. 105–125 (1979).
[16] Kobayashi, H., Distribution of seismic intensity and seismic disaster by Izu-Oshima-Kinkai earthquake, In Report of a synthetic study of the disaster caused by the 1978 Izu-Oshima-Kinkai earthquake, pp. 58–60 (1978) [Japanese].
[17] Hakuno, M., Fujino, Y., and Katada, T., A report on the damage to Civil Engineering Structures Caused by the Izu-Oshima-Kinkai earthquake of 1978, Bull. Earthq. Res. Inst. Univ. Tokyo, Vol. 53, pp. 1101–1133 (1979) [Japanese].
[18] Usami, T., Comprehensive Bibliography of Disasterous Earthquakes in Japan, Univ., Tokyo Press, p. 327 (1975) [Japanese].
[19] Sharpe, C.F.S., Landslides and Related Phenomena, Pageant Books Inc., (Columbia Univ. Press, New York), p.137 (1938).
[20] Harrison, J.V. and Falcon, N.L., Collapse structures, Geol. Mag., Vol. 71, pp. 529–539 (1934).
[21] Institute of Geology and Paleontology of Tohoku University, Phenomena and Disasters Associated with Earthquakes, Tohoku Univ. Inst. Geol. Pal. Contr., no. 67, pp. 1–99 (1969) [Japanese].
[22] Koide, H., Study of Disasters: those that occurred in mountainous regions in 1950, The Forestry Agency of Japan, p. 75 (1951) [Japanese].
[23] Morimoto, R., Ossaka, J. and Fukuda, T., Geology of the Imaichi district with special reference to the Earthquake of Dec. 26, 1949 (III), Bull. Earthq. Res. Inst. Univ. Tokyo Vol. 29, pp. 359–375 (1957).
[24] Otsuka, K. and Kimiya, K., The Landslide at Nakagi triggered by the 1974 Izu-Hanto-Oki earthquake and alteration of basement rocks, Proc. 11th Symp., Nat. Disast. Sci., pp. 162–163 (1974) [Japanese].
[25] Morimoto, R., Geology of the Imaichi district with special reference to the earthquake of Dec. 26, 1949 (II), Bull. Earthq. Res. Inst. Univ. Tokyo, Vol. 29, pp. 349–358 (1951).
[26] Murai, I., A report on damage by and seismic intensity of the Kawazu earthquake in 1976, Bull. Earthq. Res. Inst. Univ. Tokyo, Vol. 52, pp. 279–284 (1977) [Japanese].

APPENDIX A

Mechanical Aspects of the Landslide at Nanamawari

Suppose an "infinite" slope with inclination θ made up of bulk unit weight ρ. Analysis of a prismatic element of materials on the "sliding surface" was made (Fig. A.1). Thus, the limit equilibrium condition is determined in two dimensions. The element has a square base with a unit length and the height $\frac{h}{\cos\theta}$.

Sliding is assumed to take place when shear stress, τ, and normal stress, σ, on the base of the element satisfy Coulomb's criterion:

$$\tau = c+\sigma \tan \phi_u \tag{1}$$

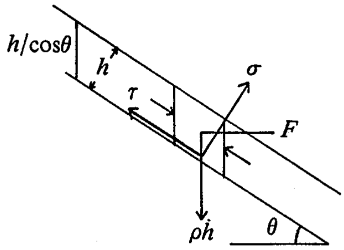

Fig. A–1 Element on the sliding surface.

in which $c=240$ gw/cm² and $\phi_u=19°$.

Usually the element receives the force of gravity and soil pressure. Soil pressure along the unslope boundary of the element is the same as that along the downslope boundary because of the "infinite" slope. Shear stress, τ, and normal stress, σ, on the base of the element are given by

$$\sigma = \rho h \cos\theta, \quad \tau = \rho h \sin\theta$$

shown graphically as point A in the σ–τ graph (Fig. A.2). If point A is in the "nonfracture range", no sliding occurs.

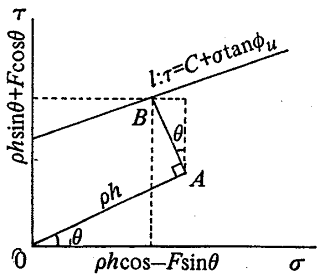

Fig. A–2 σ–τ graph.

Assuming a force, F, is exerted statically on the element in a horizontal direction by the earthquake (Fig. A.1), shear stress, τ, and normal stress, σ, on the base of the element are given by

$$\sigma = \rho h \cos\theta - F \sin\theta \tag{2}$$

$$\tau = \rho h \sin\theta + F \cos\theta \tag{3}$$

To obtain the value of F sufficient to cause sliding, substitute Eqs. (2) and (3) for Eq. (1):

$$F = \frac{c + \rho h(\cos\theta \tan\phi_u - \sin\theta)}{\cos\theta + \sin\theta \tan\phi_v} \tag{4}$$

The value of F also can be obtained by a graphical solution (Fig. A.2). Draw a line perpendicular to line OA from point A. Let the intersection of the perpendicular and fracture line 1 be B. The value of F is the length of AB.

The acceleration, α, to generate force F is given by

$$980F = \rho h s \alpha$$

in which s is 1 cm², and the units F, ρ, h, and α are gw, g/cm³, cm, and cm/s².

From this point the actual value of α is obtained by graphing on the assumption that the inclination θ of the slope is 20° to 30°, that the bulk unit weight of the materials is between 1.3 and 1.5 g/cm³ and that the thickness of the element is between 300 and 350 cm.

All the points in Fig. A.3 (P, Q, R, S, and M) show the stress on the base of the element when θ, h, and ρ have the following values.

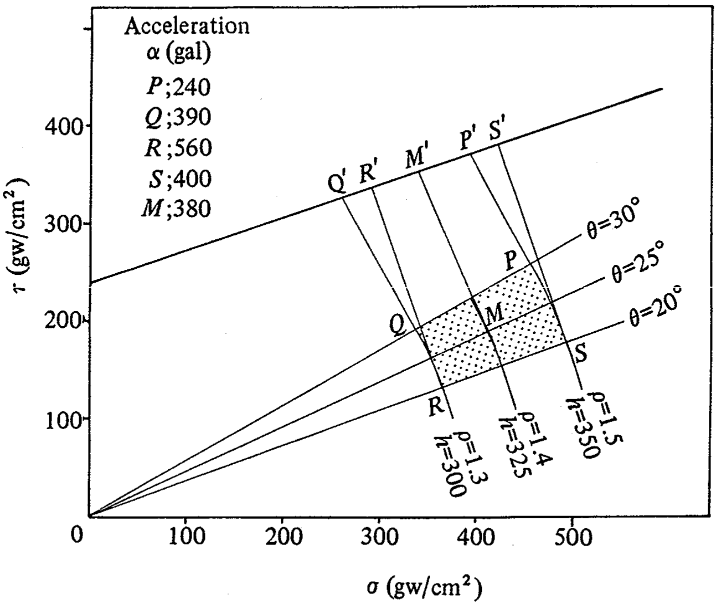

Fig. A–3 Graphic resolution of slope stability.

P : $\theta = 30°$, $h = 350$ cm, $\rho = 1.5$ g/cm^3

Q : $\theta = 30°$, $h = 300$ cm, $\rho = 1.3$ g/cm^3

R : $\theta = 20°$, $h = 300$ cm, $\rho = 1.3$ g/cm^3

S : $\theta = 20°$, $h = 350$ cm, $\rho = 1.5$ g/cm^3

M: $\theta = 25°$, $h = 325$ cm, $\rho = 1.4$ g/cm^3

Accordingly, the stress on the base of the element was in the shaded zone in Fig. A.3 before the earthquake. Point M is about in the middle of the shaded zone.

Graphing produced the following values of acceleration needed to cause sliding:

P...240 gals, Q...390 gals, R...560 gals,
S...400 gals, and M...380 gals.

The greatest value of α is 560 gals and the least value 240 gals. The value determined from point M is 380 gals.

Now, consider the seismic intensity at Mitaka-iriya during past large earthquakes recorded from the early part of the 18th century. Their isoseismals are shown in Fig. A.4 on the seismic scale of the J.M.A., in which the 5th degree closely corresponds to 80–250 gals and the 6th degree to 250–400 gals. The maximum seismic intensity at Mitaka-iriya was at the 6th degree during the 1923 Kanto earthquake, and the 5th degree, or less, during the other earthquakes. The largest horizontal acceleration at Mitaka-iriya during the Kanto earthquake presumably was smaller than the value (about 380 gals) that causes sliding.

In contrast, the largest horizontal acceleration during the 1978 earthquake at Mitaka-iriya was estimated as 400–450 gals from the survey of toppled tombstones [15]. This accounts for the 1978 sliding at Nanamawari in Mitaka-iriya being caused by the earthquake, even though the above discussion assumes an "infinite" slope and a static force provided by the earthquake.

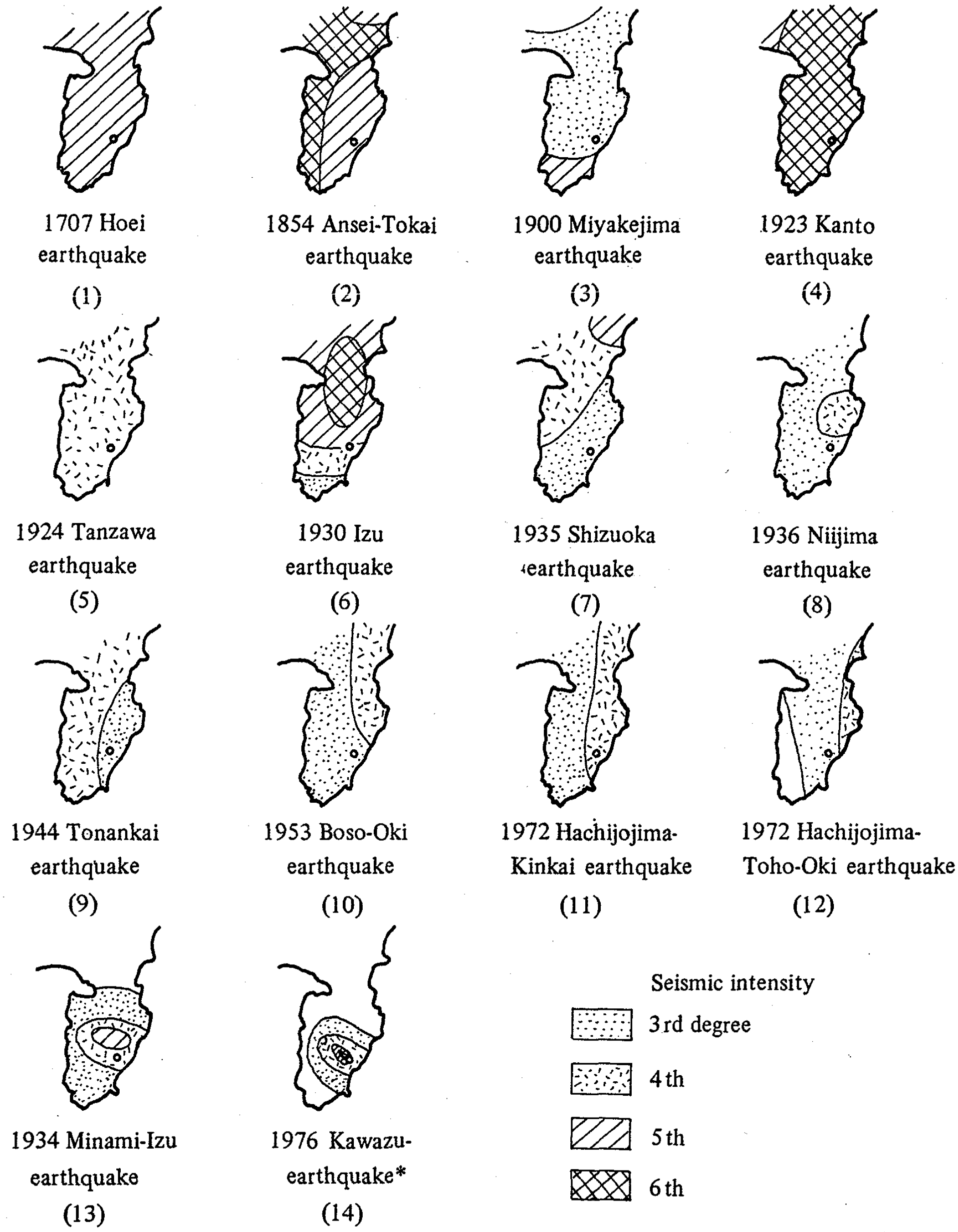

Fig. A–4 Isoseismals of past large earthquakes in the Izu Peninsula. Mitaka-iriya is shown by the open circle. The figure marked * is from Murai [26]; all the others are reproduced from Usami [18].

APPENDIX B

Mineralogical Features of the Paleosol

The mineral composition of the paleosol was checked in nonslide areas (see Fig. 1) as well as at Nanamawari. At the latter site, the beds are composed of talus deposits of andesitic rubble, the paleosol, scoria, and soil in ascending order (Fig. B.1). These beds are all outcrops in one cross section, and offer a good site for the systematic sampling needed to determine the mineralogical features of the paleosol and the other beds.

Several tens of samples were collected at the outcrop (closed circles in Fig. B.1) for X-ray and chemical analyses. Results are shown in Figs. B.1, B.2, and B.3; Fig. B.1 shows the zonation of the mineral composition. Fig. B.2 shows the relative abundance of each constituent

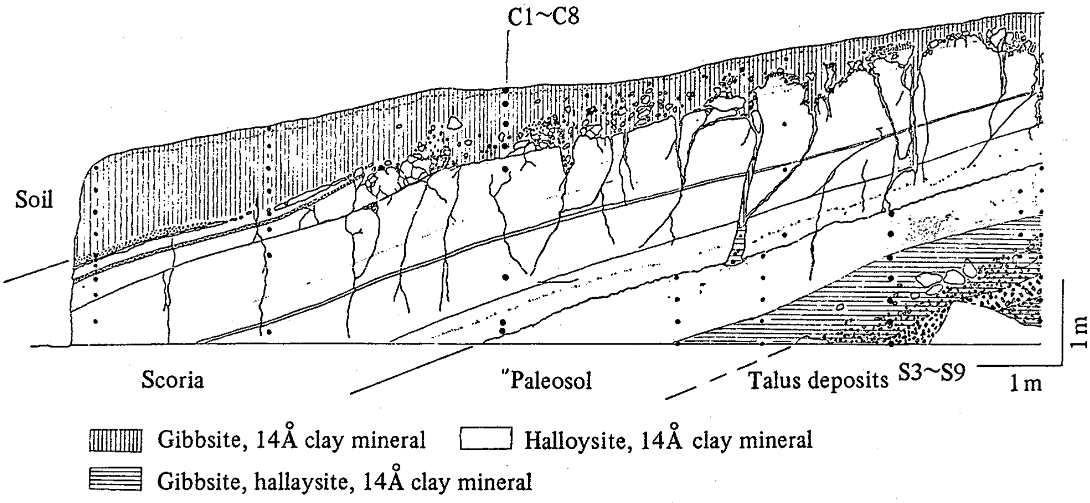

Fig. B–1 Sketch of the outcrop showing the compositional zonation of minerals. Solid circles indicate the sampling points used for X-ray analysis. C1 to C8 and S3 to S9 correspond to the points in Fig. B–2 and B–3.

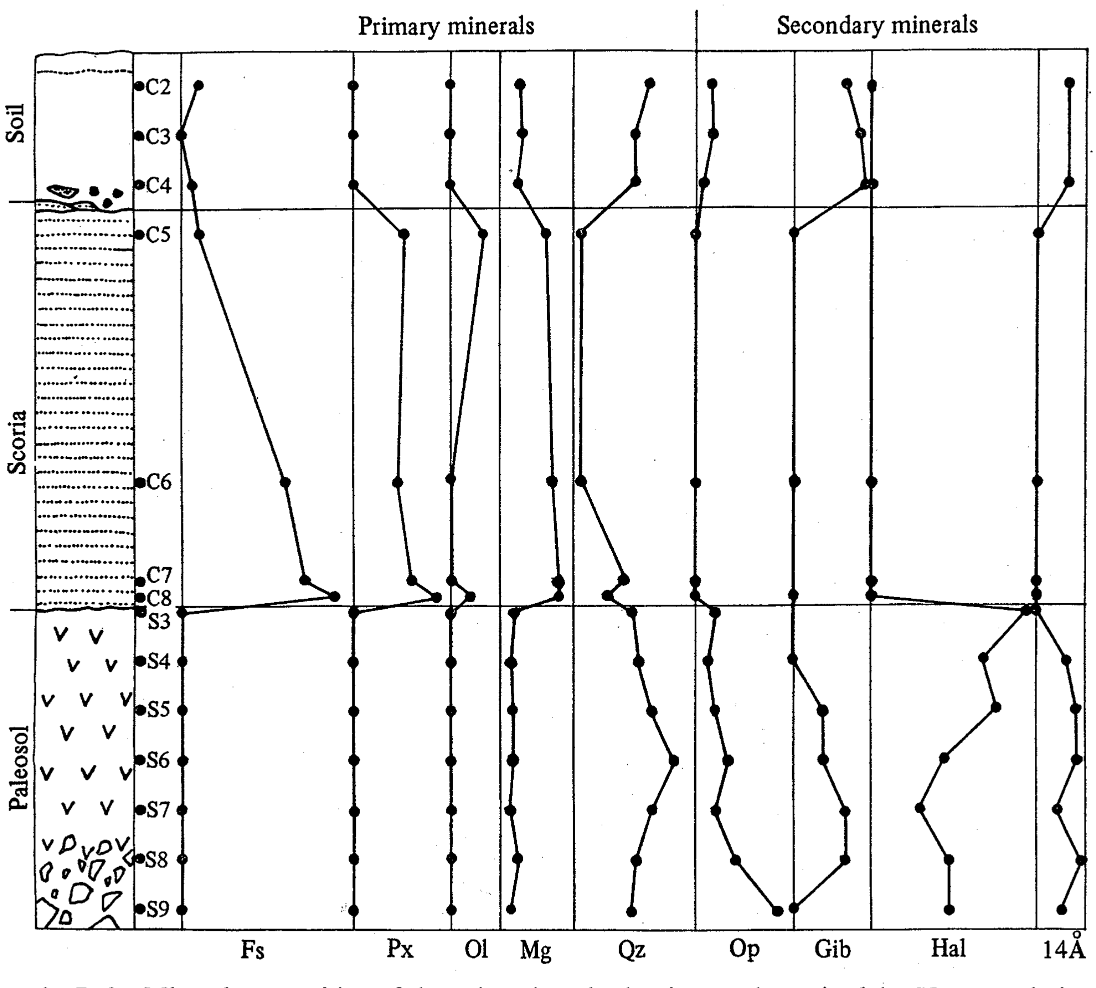

Fig. B–2 Mineral composition of the paleosol, and other layers, determined by X-ray analysis. The relative abundance of a mineral in one sample compared to that in an other sample was measured qualitatively from the prominent X-ray diffraction peaks of that mineral. Fs: feldspar (3.22 Å), Px: pyroxene (2.99 Å), Ol: olivine (2.46 Å), Mg: magnetite (2.53 Å), Qz: quartz (3.34 Å), Op: opal (4.04 Å), Gib: gibbsite (4.84 Å), Hal: halloysite (10.16 Å), and 14 Å: 14 Å clay mineral (14.48–14.24 Å).

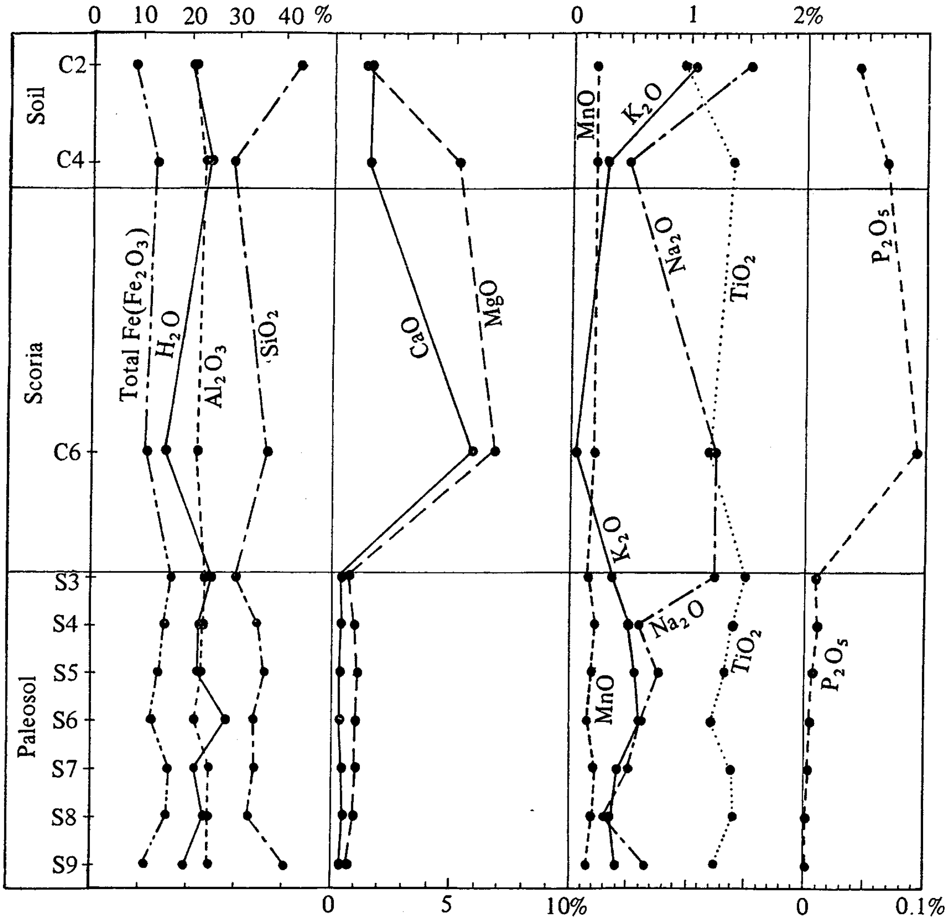

Fig. B–3 Chemical composition of the paleosol and other layers.

mineral determined from X-ray diffraction diagrams. Fig. B.3 shows the chemical composition.

In the paleosol there is zonation of mineral composition of secondary minerals that resembles the zonation in the landslide area at Nanamawari. The upper part is rich in halloysite with a subordinate 14 Å clay mineral but is without gibbsite. The lower part is rich in gibbsite with subordinate halloysite and a 14 Å clay mineral. Besides these, opal (probably a secondary mineral), quartz, magnetite, and sometimes feldspar are present. The relative abundance of gibbsite seems to be in proportion to that of opal, and to be in inverse proportion to that of halloysite (Fig. B.2).

The scoria above the paleosol includes secondary minerals scarcely, but contains feldspar, pyroxene, olivine, magnetite, and quartz. The structure of soil at the top indicates that it is formed by the weathering of the scoria underneath (Fig. B.1). This soil contains quartz, magnetite, gibbsite, opal, a 14 Å clay mineral and some feldspar. Pyroxene and olivine probably have been extenguished by weathering.

The main difference between the paleosol and the present soil is that the paleosol contains halloysite, whereas the soil does not. Assuming that the paleosol was formed primarily with the same mineral composition as that of the present soil, the halloysite must have been formed later probably by chemical reaction between the primary paleosol and water percolating from the surface. The relatively large amount of halloysite in the upper part of the paleosol as compared to the lower part supports this hypothesis.